Cell
Leading Edge

CellPress
OPEN ACCESS

Review

Parsing patterns: Emerging roles of tissue self-organization in health and disease

Raul Ramos,[1,2,3] Benjamin Swedlund,[4] Anand K. Ganesan,[5,6] Leonardo Morsut,[4,7] Philip K. Maini,[8] Edwin S. Monuki,[2,9] Arthur D. Lander,[1,5,*] Cheng-Ming Chuong,[10,*] and Maksim V. Plikus[1,2,3,5,*]

[1]Department of Developmental and Cell Biology, University of California, Irvine, Irvine, CA, USA
[2]Sue and Bill Gross Stem Cell Research Center, University of California, Irvine, Irvine, CA, USA
[3]NSF-Simons Center for Multiscale Cell Fate Research, University of California, Irvine, Irvine, CA, USA
[4]Eli and Edythe Broad CIRM Center, Department of Stem Cell Biology and Regenerative Medicine, Keck School of Medicine, University of Southern California, Los Angeles, CA, USA
[5]Center for Complex Biological Systems, University of California, Irvine, Irvine, CA, USA
[6]Department of Dermatology, University of California, Irvine, Irvine, CA, USA
[7]Alfred E. Mann Department of Biomedical Engineering, Viterbi School of Engineering, University of Southern California, Los Angeles, CA, USA
[8]Mathematical Institute, University of Oxford, Oxford, UK
[9]Department of Pathology and Laboratory Medicine, University of California, Irvine, Irvine, CA, USA
[10]Department of Pathology, Keck School of Medicine, University of Southern California, Los Angeles, CA, USA
*Correspondence: adlander@uci.edu (A.D.L.), cmchuong@med.usc.edu (C.-M.C.), plikus@uci.edu (M.V.P.)
https://doi.org/10.1016/j.cell.2024.05.016

SUMMARY

Patterned morphologies, such as segments, spirals, stripes, and spots, frequently emerge during embryogenesis through self-organized coordination between cells. Yet, complex patterns also emerge in adults, suggesting that the capacity for spontaneous self-organization is a ubiquitous property of biological tissues. We review current knowledge on the principles and mechanisms of self-organized patterning in embryonic tissues and explore how these principles and mechanisms apply to adult tissues that exhibit features of patterning. We discuss how and why spontaneous pattern generation is integral to homeostasis and healing of tissues, illustrating it with examples from regenerative biology. We examine how aberrant self-organization underlies diverse pathological states, including inflammatory skin disorders and tumors. Lastly, we posit that based on such blueprints, targeted engineering of pattern-driving molecular circuits can be leveraged for synthetic biology and the generation of organoids with intricate patterns.

INTRODUCTION

Patterns are prevalent in the biological world, occurring at all levels of organization, from macromolecular assemblies to multicellular collectives. Patterns manifest both as periodic elements in space and sequences of events in time[1] and commonly emerge through self-organization. This captivating process relies on local interactions between components of an initially disordered system, with each component following simple rules. Oftentimes, such "bottom-up" self-organization works within boundaries set by "top-down" global coordinates to generate an extraordinary array of patterns. Contribution of self-organization manifests itself most notably in developing tissues. But it is also apparent in some diseases, where tissues may develop remarkable pathological patterns, possibly reflecting loss of physiological constraints on patterning or selective self-organization to the advantage of malignant cells.

Hereafter, we discuss why biological systems display patterns so frequently and whether they obey mathematically simple rules, such as Turing rules, thought to underlie pattern self-organization in initially homogeneous systems whose cells respond to differentially diffusing signaling factors.[2] We also discuss how bottom-up self-organization works together with initial top-down conditions to stereotype tissue patterns, when and why adult tissues exhibit propagating waves, and how patterns emerge *de novo* upon regeneration. We explore why patterns emerge frequently upon disease and how studying pattern formation could inform pathogenic cellular and signaling mechanisms. Lastly, we investigate if we can learn to synthesize precise patterns *in vitro* to enable tissue bioengineering.

COLOR PATTERNS—MORE THAN MEETS THE EYE

Periodic patterns, such as spotted and striped fur coats in big cats (Figure 1A),[3] QR-code-like scales in lizards (Figure 1B),[4] or spiral fingerprints in humans (Figure 1C),[5] often inspire art and fashion. The ability of computer algorithms to simulate patterns like these has long suggested that self-organizing molecular processes can, in principle, partition naive animal tissues into periodic structures. Yet, skepticism remains as to whether embryonic processes that produce them are truly self-organized

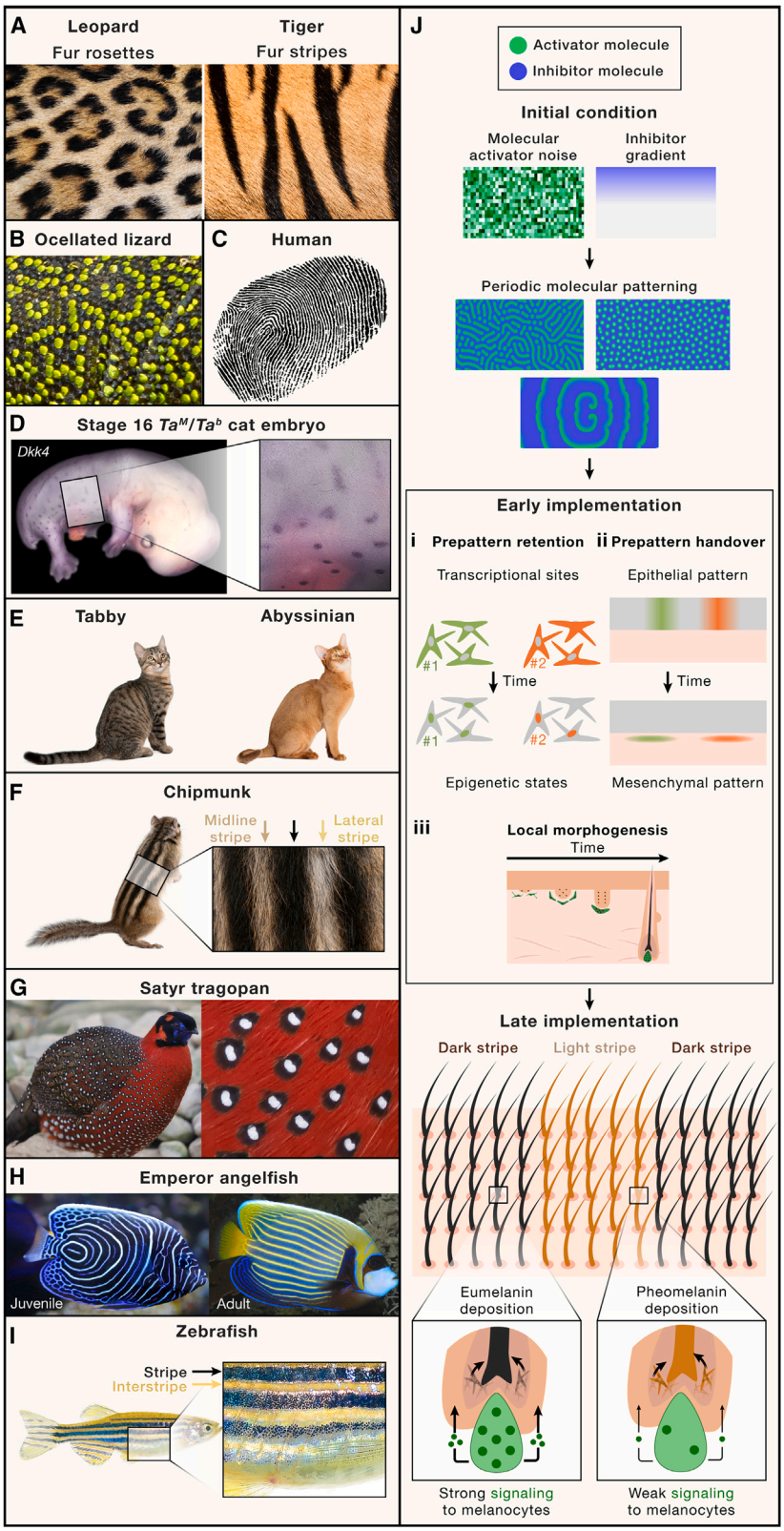

Figure 1. Skin patterns and their mechanisms

(A) Periodic fur coloration patterns in the form of spots and rosettes in leopards and stripes in tigers.

(B) QR code-like scale coloration pattern in ocellated lizard.

(C) Labyrinthine pattern of epidermal ridges in a human digit tip.

(D) *Dkk4* expression reveals its periodic epidermal pattern in stage 16 Ta^{M}/Ta^{b} (mackerel tabby) domestic cat embryo.

(E) Genetic alterations to *Dkk4* produces differential fur markings as seen in domestic tabby vs. abyssinian cats.

(F) In chipmunks, alternating light and dark fur stripes produce a stereotyped skin coloration pattern.

(G) In the satyr tragopan, a spotted plumage coloration pattern emerges collectively from individually patterned feathers.

(H) Dynamically evolving skin coloration patterns in emperor angelfish. Typical patterns in juvenile (left) and adult animals (right) are shown.

(I) Periodic pigment stripe pattern in zebrafish skin. Selected stripes are magnified and annotated on the right.

(J) Conceptual representation of fur coloration pattern emergence and implementation. First, a differential distribution of molecular activators (green) and inhibitors (blue) establishes an initial condition that constrains pattern outputs. R-D mechanisms then give rise to spatially distributed patterns of activator and inhibitor molecules. During the early implementation stage, collective cellular behaviors stabilize molecular prepattern information: (i) the latter can become stably retained within cells as epigenetic memory, (ii) initially patterned cells can hand over information to another cell type for "safekeeping," and (iii) local morphogenesis can advance tissue to a new stable morpho-functional state. Lastly, late implementation occurs through differential cell activities in molecularly patterned tissue units.

Images for Figure 1D were kindly provided with permission by Kelly McGowan and Gregory Barsh.

or, rather, highly constrained and stereotyped by other phenomena, such as initial conditions and boundaries.

Skin coloration patterns are perhaps some of the most studied examples of biological self-organization. Light-colored fur coats in felines often feature periodic dark stripes, spots, rosettes, and blotches—patterns that frequently emerge in computer simulations of Turing-type models, in which interactions between at least two differentially diffusing signaling molecules can be sufficient to induce target cells into a spatially periodic pattern even from an initially random state.[6] Each periodically colored skin region contains differentially pigmented hair follicles, whose mesenchymal cells secrete variable quantities of Endothelin-3 that regulates black vs. yellow pigment production by melanocytes.[3] Thus, coat coloration patterns are driven by a patterned mesenchymal signal encoded in embryogenesis. Intriguingly, within early-stage embryonic skin, which consists of a layer of epithelial cells on top of fibroblast-rich mesenchyme, coat-color encoding occurs within the epithelium rather than mesenchyme, days prior to hair development.[7] Embryonic epithelium develops periodic stripes and spots of alternating thickness, with darkly pigmented hairs eventually forming at sites of thicker epithelium.[8] Compared to thin regions, epithelial cells from thick stripes and spots express high levels of soluble WNT pathway factors, both activators, such as WNT ligand molecules, and their inhibitors, such as DKK molecules (Figure 1D), that physically interfere with WNT ligands' binding to cell surface receptors. Theoretically, molecular interactions of short-range WNT agonists and long-range antagonists can implement Turing-like patterns[7]—a possibility supported by spotless cats (Figure 1E) carrying inactivating mutations in WNT antagonist *Dkk4*.[8] Interestingly, epithelial thickness patterns in cat embryos recede prior to hair morphogenesis, suggesting an as-yet-unknown epigenetic mechanism for pattern memory retention in these tissues and a signaling mechanism for epithelium-to-mesenchyme information "handover." This example suggests that complex biological patterns may acquire spatial instructions from a "pre-pattern" that itself self-organizes within a morphologically naive tissue (Figure 1J).

Unlike felines, African striped mice, chipmunks (Figure 1F),[9] and quails[10] feature stereotypical skin coloration patterns with a precise number of stripes along the midline. Such patterns can arise when an initial condition, such as a signaling gradient, constrains a stochastic Turing system.[11] In African striped mice, two light lateral stripes are prominently pale, caused by lack of pigment along most of the hair length.[9] This is foreshadowed in the embryonic epidermis by an initial condition in the form of symmetric streaks of *Alx3* expression. Pale hair-making follicles continue to express *Alx3*, where it suppresses melanocyte differentiation by inhibiting master-regulator gene *Mitf.* Symmetry-breaking *Alx3* expression can be, in principle, instructed by the signaling effects of either centrally positioned neural tube or bilaterally symmetric somites. An analogous initial condition, which features variably colored feather stripes, has evolved in quails. The latter arise in embryonic skin regions with varying mesenchymal expression of *Agouti*,[10] which instructs differential pigment synthesis by melanocytes within feathers. Thus, in addition to self-organizing pre-pattern, complex biological patterns can involve an initial condition that stereotypes Turing-like outputs (Figure 1J).

Pigment pattern implementation in mammals and birds is highly discrete because their hair and feather follicles, respectively, compartmentalize melanocytes and regulate color production autonomously. In addition, individual follicles can modulate their melanocyte activity over time of growth, producing multicolored appendages—either hairs or feathers,[12] which, when combined, give rise to mosaic coloration patterns (Figure 1G). However, in fishes and reptiles, whose skin lacks discontinuous appendages, discrete coloration is challenging because pigment-making cells can move about unobstructed. Yet, emperor angelfish (Figure 1H) and zebrafish (Figure 1I) form discrete, dynamically evolving or temporally stable skin coloration patterns, respectively. In zebrafish, a periodic pigment stripe pattern is generated upon spatial segregation of black melanophores and yellow xanthophores. Cells segregate in response to short-range activating and long-range inhibitory interactions that collectively satisfy a Turing principle.[13] Indeed, at short distances, melanophores and xanthophores suppress each other's survival, while at long distances xanthophores promote the survival of melanophores.[14] Interestingly, while zebrafish stripe patterns mathematically behave like a reaction-diffusion (R-D) system, they are not underpinned by diffusible morphogens. Instead, they are driven by differential cell proliferation, migration, and survival, guided by discrete melanophore-to-xanthophore interactions via signal bearing short and long cellular projections.[13] Discrete coloration can also arise in certain reptiles even though their skin scales are continuously connected. Indeed, scales in ocellated lizards are monochromatic: black-only or green-only, housing mainly melanin-containing melanophores or light-reflecting iridophores, respectively.[4] Intriguingly, sharp coloration patterns of adult lizards begin as blurry patterns in juveniles and evolve over time via a contrasting process, whereas multicolored scales become monochromatic, and others switch color from black to green or vice versa (Figure 1B). A cellular automaton model can simulate the skin color sharpening observed in lizards, assuming that each scale maintains or changes its color by accounting for its own original color and that of its nearest-neighbor scales.[4] Yet, how discrete cellular behavior emerges across anatomically continuous tissue remains undetermined. One possibility is that continuous R-D interactions among pigment cells significantly weaken at notably thinner scale boundaries.[15] Theoretically, anatomical thinning can diminish paracrine or direct contact-based interactions between cells, which individual scales can interpret in a binary way and then sum binary inputs from all nearest-neighbor scales. A precise mechanism aside, this example suggests that self-organizing processes engage in biological pattern-formation both early, to pre-pattern naive tissues, and late, to refine imprecise patterns (Figure 1J). As Turing himself stated, "Most of an organism, most of the time is developing from one pattern into another, rather than from homogeneity into a pattern."[2]

WHY DO PATTERNS EXIST SO PREVALENTLY?

Animals display periodic morphological, metabolic, and transcriptional activity patterns across a broad range of spatial and

temporal scales. Examples are ample and include intestinal epithelium with a carpet-like array of villi, liver with mosaic-like hexagonal lobules, and lung with periodically branched alveoli. Most of the time, biologists ask how patterns emerge as they strive to understand underlying mechanisms. Yet, asking why periodic patterns are so frequent is equally important. Understanding why biological systems commonly opt for self-organized patterning as a morphogenetic force can yield both mechanistic and evolutionary insights.

Overcoming limits on communication

Self-organization can improve molecular communication between cells as they coordinate with one another. Like all forms of communication over space, biochemical communication is constrained by signal-to-noise ratio,[16] and cells efficiently relay diffusible morphogens only at relatively short distances not exceeding several hundred μm. Beyond that, declining signals become masked by noise[17]; yet, most animal tissues efficiently operate on centimeter and even meter scales. To overcome the divide between molecular gradient scale, which is microscopic, and physical tissue scale, which can be meters long, biological systems repetitively pattern themselves into small units. Within such small units, cells can then efficiently interact, minimally affected by noise interference (Figure 2A). For example, despite vast size differences between mouse and human liver, individual liver lobules only differ by a factor of two: ∼500 μm in mice and ∼1,000 μm in humans.[18] Importantly, while patterning improves molecular communication, additional solutions exist to extend it beyond the ∼1 mm range. These include deployment of long-range cellular projections, migrating signal-carrying cells, electrical cell-to-cell coupling, etc.

Increasing robustness

Patterned tissues are more resistant to catastrophic loss of function. In vertebrate skin, densely patterned arrays of appendages offer robust protection and thermoregulation, and loss of even thousands of them may not significantly reduce fitness. For example, an average human has approximately 100,000 hair follicles on the scalp,[19] and hair loss becomes clinically perceivable only when hair density drops by over half (Figure 2B). In densely haired animals, such as mice, healing of wounded skin commonly occurs with a hairless scar yet without a perceived breach in fur coat due to naturally high density of peri-wound hairs that cover the scar (Figure 2C). Such compensation by peri-wound hairs fails only when wounds become substantially large, in which instance the healing process triggers neogenesis of new follicles[20] that aid in patching breached pelage. Moreover, at least some actively maintained and dynamically calibrated patterns, such as pigment stripe patterns in zebrafish, are robust to perturbation—they autonomously regenerate after disruption, such as upon pigment cell ablation.[14]

Diversifying functions

Patterning also enables anatomical and functional diversification of individual tissue units. For example, most mammals feature morphologically distinct teeth—incisors, canines, and premolars/molars—tasked with cutting, tearing, and crushing food, respectively. Birds grow diverse feather types, including bilaterally symmetric and asymmetric feathers on the wings and the tail, radially symmetric downy feathers on the body, and various mixed feather forms, each adapted for flight, thermoregulation, and display, among other functions.

Typically, diversification occurs during pattern implementation rather than pattern self-organization. Indeed, at early stages of morphogenesis, all teeth depend on the same molecular regulators, including SHH, FGF, WNT and BMP pathways, and appear morphologically similar. However, during the so-called bell stage, molars diverge from incisors and form secondary enamel knots that initiate multi-cusp crown patterning. In birds, implementation of diverse feather morphologies also occurs after initial follicle morphogenesis. For instance, bilaterally symmetric feathers form WNT-dependent shafts,[21] while flight feathers become additionally asymmetric in a retinoic-acid-dependent mechanism.[22] Notably, an early molecular event, if remembered by cells as stable gene expression, can restrict program implementation at a given body location. One such example is striped skin coloration in cats, which depends on a self-organized epidermal WNT pre-pattern, epithelium-to-mesenchyme information transfer, and its "memorization" as stable Endothelin-3 expression by follicle fibroblasts.[3,8] Likewise, in developing bird wings, transient anterior-posterior SHH gradient becomes "memorized" by lateral plate mesenchyme as stable expression of SIM1 and ZIC1/2/3. The latter are necessary for implementing bilaterally asymmetric shaping of flight feathers along the wing margin.[23]

Enabling coexistence of incompatible states

Commonly, patterning results in physical segregation of cell states, which is then actively maintained by stabilizing events. Such segregation enables coexistence and collaboration between otherwise incompatible cell states. For example, stem cells and their differentiated progenies are often incompatible and frequently occupy distinct tissue micro-domains. In mouse intestine, epithelial stem cells occupy 100-μm-deep crypts, while their progeny—enterocytes and tuft, goblet, and enteroendocrine cells—occupy the adjacent 300-μm-high villi.[24] Such sub-millimeter distances are sufficiently large to segregate incompatible environments of the crypt, where high levels of WNT signaling promote long-term stemness (i.e., the ability of stem cells to self-renew), and that of the villus, where high levels of BMP signaling promote enterocyte differentiation.[25] And yet, despite the long distance between the crypt and the villus, stem cells can still move up and differentiate and allow feedback regulation.

In the liver, repetitive lobules form around central veins (CVs), with hepatocytes radially self-organizing around them into distinct peri-central, mid-lobular, and peri-portal transcriptional, metabolic, and signaling states (Figure 2D). Peri-central hepatocytes are glycolytic, lipogenic, and ketogenic and exist in high-WNT-signaling environments. In contrast, peri-portal hepatocytes undergo β-oxidation and gluconeogenesis and operate in a low-WNT-signaling state. The High-WNT-signaling status of peri-central hepatocytes depends on soluble WNT agonist R-spondin3, secreted by CV endothelial cells.[26] R-spondin3 gradient-dependent patterning minimizes interference between metabolically distinct hepatocytes of the lobule, while small

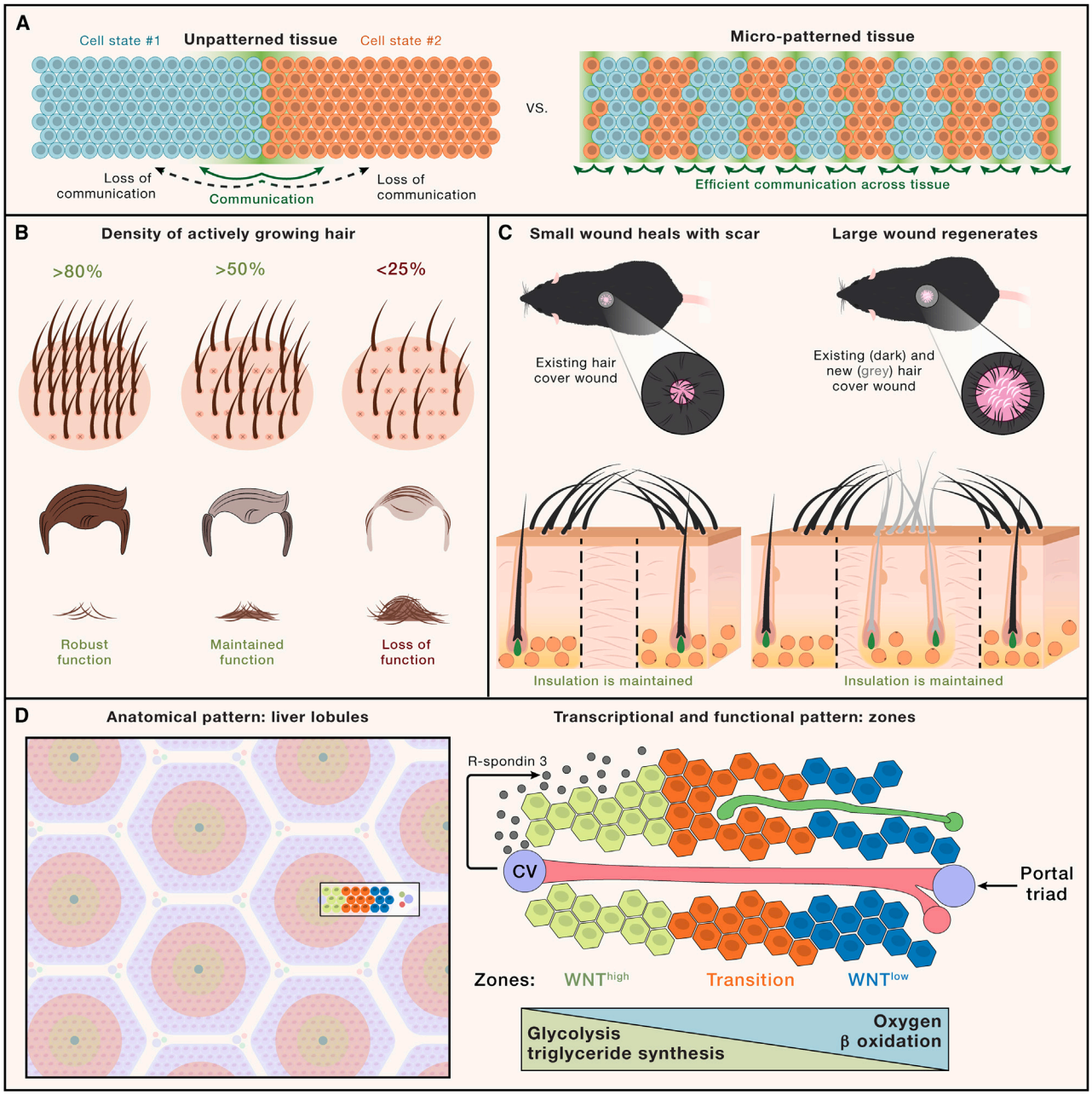

Figure 2. Possible reasons behind the prevalence of patterning in biology

(A) Illustration of how micro-patterning of cell collectives into sub-millimeter size units enables efficient tissue-wide communication (green gradients in right graphic) without significant noise interference that would otherwise afflict un-patterned tissues (left graphic).

(B) Top row illustrates magnified skin with active follicles (black hairs) and inactive follicles (asterisks). Bottom row illustrates corresponding scalp hair coverage. Robust function can be achieved by producing large numbers of individual patterned tissue elements. Protection of human scalp skin from solar radiation is achieved by forming many (~100,000) hair follicles, each growing a long hair fiber. In healthy adults, ~80% of growing follicles provide robust scalp coverage (left). In adults with alopecia, naturally high follicle density buffers against loss of scalp coverage, even if only ~50% of them are actively producing hair (middle).

(C) Following skin wounding in mice, protective and thermoregulatory functions of the fur are preserved either through numerous pre-existing hairs at wound edges when wounds are small (left) or through *de novo* formation of more hair follicles in the center of large wounds (right). Skin "measures" wound dimensions, regenerating new follicles only in large wounds.

(D) Metabolically incompatible cell states become segregated in liver lobules, where hepatocytes organize across oxygen and nutrient gradients. Hepatocytes near the central vein (CV) experience low oxygen and maintain elevated glycolysis and triglyceride synthesis rates. CV-secreted R-spondin 3 sustains high WNT signaling and corresponding distinct transcriptional state by hepatocytes (green). In contrast, hepatocytes near portal triad (blue) exist in a low WNT environment, entering an alternative transcriptional state compatible with an oxygen-rich environment and optimized for β-oxidation and gluconeogenesis.

overall lobule size enables efficient diffusion-based sharing of end-product metabolites between segregated hepatocyte states.

Therefore, self-organized patterning has been adapted by biological systems: (1) to efficiently partition tissues into groups of cells small enough to maintain efficient diffusion-based molecular communication, (2) to generate multiple replicates of identical tissue units and then (3) diversify their morphology for expanded function, and (4) as a solution for segregating functionally essential yet incompatible cell states.

WHY IS SELF-ORGANIZATION A FUNDAMENTAL MECHANISM?

There can be many reasons for why self-organization became an evolutionary preference for forming patterns. Self-organization via the Turing mechanism is inherently simple, requiring just three components: (1) a positive feedback loop, (2) a negative feedback loop, and (3) agent(s) that couple them over space.[2] Diffusible signaling molecules are ubiquitous in biological systems, offering numerous solutions to feedback-loop coupling. Self-organizing patterns may be seen as spatial analogs of feedback oscillations in time, which themselves only require a negative feedback loop and a delay around it.[27] Such oscillatory networks can function within a single cell, as in the case of the circadian clock.[28] However, such networks can also produce Turing patterns when an inhibitor disproportionately delivers feedback to an activator at a location different from where the inhibitor was originally produced. Cellular oscillations presumably evolved early in biological systems. Notably, spatial oscillations emerge both in prokaryotes[29] and unicellular eukaryotes[30] that assemble into collectives. *Dictyostelium discoideum* amebas can assemble into fruiting bodies via a self-organized patterning process driven by cAMP oscillations in time and space and chemotactic responses to it.[31] We posit that existing feedback loops became rapidly deployed upon the evolution of multicellularity to enable pattern-based solutions to novel challenges—partitioning cells into distinct, yet cooperating, units. Once diffusible signaling molecules emerged, existing feedback loops could have been re-deployed essentially unchanged to produce self-organizing patterns.

Self-organizing processes are inherently versatile, and a majority of observable biological patterns—both motionless, standing wave patterns and dynamic, moving wave patterns—can be mathematically described by similar sets of Turing equations.[32] Therefore, a given biological system can produce a variety of static and dynamic patterns by simply adjusting parameter values for a few molecular components without inventing new components. Adjusting parameter values, such as a soluble factor's diffusion properties, is also sufficient to quickly and reversibly turn pattern-forming regime on and off[33]—a phenomenon rooted in the fact that a single set of Turing equations can have both pattern-forming and pattern-less solutions, depending on the parameters of its interacting elements. Self-organized patterning is compatible with additional patterning mechanisms and can be effectively combined with numerous local or global initial conditions and boundary constraints, producing stereotyped patterns with globally changing features—unidirectional stripes, specific number of stripes, or bilaterally symmetric stripes.[34]

BUILDING BODIES WITH PATTERNS

Patterning requirements for morphogenetic processes depend on specific developmental scenarios. While in some instances, such as hair morphogenesis, a large yet imprecise number of patterned elements matters the most (the average adult human has approximately five million hairs). In other scenarios, such as hand morphogenesis, a precise number of patterned elements and their spatial arrangement are crucial (a hand has five fingers). To accommodate diverse pattern demands, self-organized processes can play out in their most classic way within naive tissue and with high stochasticity or, instead, overlay on pre-existing constraints for more stereotyped outputs.

Vertebrate skin is covered by a large number of patterned appendages—hairs, feathers, or scale—whose morphogenesis in embryonic skin critically relies on self-organizing mechanisms. In mice, hair morphogenesis occurs in consecutive waves, with the earliest-born hair primordia, called placodes, emerging on embryonic day (E) 14. Placode position is set forth by WNT signaling, which self-organizes into a labile pre-pattern mediated by short-acting WNT ligands and long-acting DKK inhibitors.[7] Such signaling pre-pattern locally instructs hair morphogenesis at sites of high WNT activity through a multi-step implementation program involving WNT stabilization via ectodysplasin pathway, BMP pathway, epithelial cell migration, and fibroblast migration to form a placode and associated mesenchymal condensate that then go on to reciprocally drive each other's differentiation toward hair fate[35] (Figure 3A). In principle, WNT-based R-D is sufficient to spontaneously pattern embryonic skin into hair primordia. Indeed, placodes emerge spontaneously in cultured embryonic mouse skin[35] or when a mixed suspension of embryonic skin cells is injected subcutaneously into host mice.[36] Yet, in actual embryos, distinct skin sites display early WNT asymmetry, where hairs form first. The earliest-born trunk hairs emerge around mammary gland primordia,[37] whose morphogenesis also depends on WNT (Figure 3B). Moreover, earliest-born (also known as "primary") hair follicles themselves become sources for WNT asymmetry and instruct subsequent follicle development. As embryonic skin expands, new hair placodes arise at equidistant sites from primary follicles, where drops in WNT antagonist levels occur the earliest[38] (Figure 3C). This example illustrates how a single pathway operating within a single cell type can generate self-organized signaling instability to initiate patterned morphogenesis. It also shows that in expanding embryonic tissues, primary pattern elements can act as signaling "anchors" instructing the location of additional pattern elements.

Feather morphogenesis in birds follows analogous pattern-forming behavior. The earliest born feather buds in chicken embryo form along the dorsal midline, where they then instruct morphologically precise patterns of additional feather buds through midline-to-flank waves of ectodysplasin signaling.[39] Flightless ostriches and emus, however, do not follow this wave-like mechanism and instead develop feather buds nearly simultaneously in an imprecise pattern.[40] Once formed, feathers instruct morphogenesis of a secondary grid-like dermal muscle

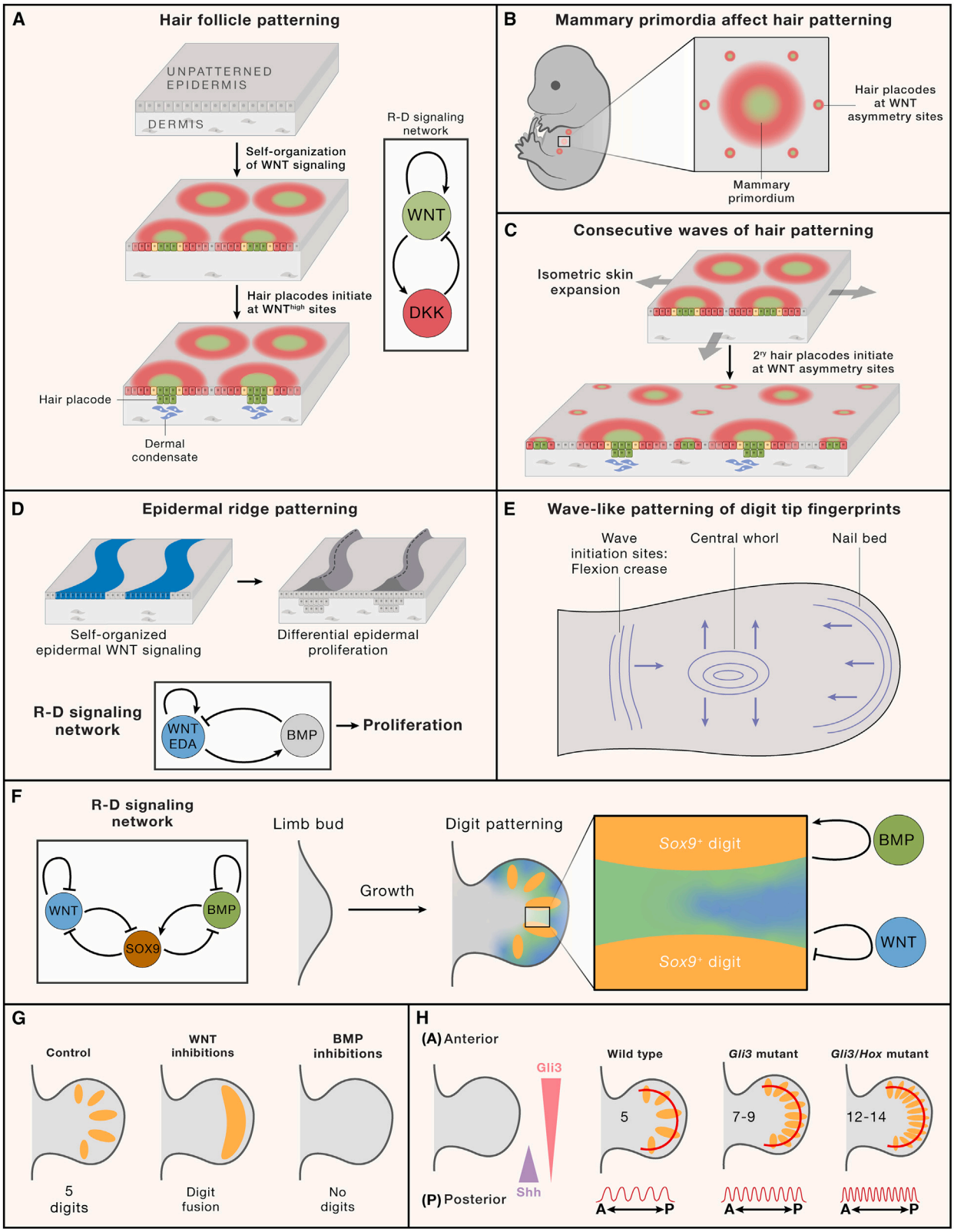

(legend on next page)

pattern. Muscle fibers in chicken skin arise around feather buds and grow radially in all directions yet become stable only if they connect to neighboring feather buds. In this way, an array of feather bud "nodes" serves as the initial condition for the dermal muscle network, stereotyping it into a grid-like nearest-neighbor configuration.[41]

Unlike haired skin, hairless skin of palms and soles in primates develops dermatoglyphic patterns of epidermal ridges that arrange into arches, loops, and whorls. The latter, when moisturized with sweat, endow skin with better grip.[42] Epidermal ridges form through a Turing-like process analogous to the previously discussed hair patterning mechanism. Size and spacing of ridges are regulated by a R-D signaling network consisting of WNT as the principal activator, WNT-amplifying ectodysplasin, and WNT-regulated BMP inhibitor.[5] Importantly, while early-stage epidermal ridges and hair placodes share numerous marker genes, they diverge at the pattern implementation stage: while hairs recruit mesenchymal condensates that help self-limit their size, ridges remain epithelial-only and arrange into continuous "lines" instead of "spots" (Figure 3D). Turing-like morphogenesis of dermatoglyphics is supported by observations in mice. Ventral skin of mouse digits features periodically spaced ridges—a murine analog of human fingerprints. Mice mutants for ectodysplasin ligand show ridge fragmentation into spots, while mice with amplified ectodysplasin receptor develop thickened ridges with enlarged spacing. Complex dermatoglyphics in human fingertips form by a wave-like morphogenesis, whereas ridges propagate from initiation sites located at the dorsal-ventral digit boundary and the inter-phalanx crease—likely sites of signaling asymmetry[5] (Figure 3E). This example shows that the same R-D signaling network can be deployed at different body sites, albeit with modifications for distinct self-organized outcomes.

Unlike in skin, where large numbers of appendages are generated at the expense of precision, in the limb, the number of digits needs to be exact. Mouse limbs have five digits, each being specified as condensations of chondrogenic cells at E12.5. Their specification is driven by a Turing-like mechanism implemented by a three-component molecular network: SOX9 and soluble ligands for BMP and WNT pathways.[43] Digit primordia become specified by high SOX9 expression, which is activated by long-range BMP2 secreted by interdigit cells. Interdigit cells also secrete short-range acting WNTs that suppress SOX9, preventing ectopic chondrogenic fate (Figure 3F). Indeed, disruption of either BMP or WNT signaling in explant cultures of E11.5 limb buds results in aberrant digit specification—digit primordia are lost upon BMP inhibition and fuse upon WNT suppression (Figure 3G).[43] Unlike their formation, per se, digit number precision requires SHH signaling. Deletion of either *Shh* or its repressor *Gli3*, which form inverse gradients along the anterior-posterior limb bud axis, causes polydactyly—supernumerary fingers or toes and loss of digit identity.[44] Polydactyly becomes exacerbated upon additional deletion of certain HOX genes such that mice lacking *Gli3*, *Hoxd11-13*, and one copy of *Hoxa13* develop 14 digits.[45] Super-polydactylous mice are reminiscent of ray-finned fishes, whose fins have multiple fan-like skeletal elements.[46] Extreme polydactyly upon HOX gene loss is accompanied by a decrease in digit periodicity (i.e., interdigit distance reduces) within an otherwise similarly sized space (Figure 3H). This suggests that a BMP/SOX9/WNT-based Turing-mechanism for digit patterning is constrained both by SHH-GLI3 and HOX genes, with the latter modulating R-D wavelength. Similar to skin color stripes, this example shows that stereotypical patterns can be underpinned by a Turing mechanism constrained by initial conditions. It also shows how signaling pathways involved in mediating reaction diffusion affect differential cell fate implementation.

Similar to digits, the number of teeth and their shapes at each jaw position in a given mammalian species needs to be precise, and yet they vary greatly across mammalian families. Molar teeth feature anatomically complex crowns whose shape is patterned by Turing-like morphogenesis.[47] Molar crown morphogenesis depends on the number and position of secondary enamel knots, which are signal-secreting clusters of epithelial cells. Paracrine activator signals, such as BMPs, induce enamel knots by promoting dental epithelial-cell differentiation. In turn, enamel knots produce inhibitory signals, including FGFs and SHH, whose opposing actions self-limit enamel knot size and drive surrounding epithelial and mesenchymal proliferation, which shapes three-dimensional crown "landscapes." Crown morphogenesis, driven by activators and inhibitors, is coupled to its physical growth, and both

Figure 3. Pattern formation during embryonic morphogenesis

(A) Illustration of hair follicle patterning. Embryonic skin, consisting of epidermis (dark gray) and dermis (light gray), is shown on the left, while key R-D signaling network components are on the right. The latter patterns embryonic epidermis into WNT^{high} areas (spots) and WNT^{low} zones (surrounding circles). Hair placodes then develop from WNT^{high} epidermis (annotated on the bottom-left graphic). Dermal condensates (blue cells) then form under placodes.

(B) The earliest hair placodes form around WNT^{low} boundaries of mammary-gland primordia. Mouse embryo is shown on the left and mammary gland primordium with hair placodes on the right.

(C) Secondary hair placodes initiate through a WNT-dependent mechanism between earlier-born placodes, as their WNT^{low} zones separate upon embryonic skin expansion.

(D) Illustration of epidermal ridge patterning in embryonic volar skin (top), consisting of epidermis (dark gray) and dermis (light gray). Key R-D components are shown at the bottom. The latter appears to pattern the epidermis into WNT^{high} ridges (blue lines), where subsequent epidermal proliferation and differentiation produce elevated ridges (dark gray protrusions).

(E) Illustration of the fingertip (gray) with epidermal ridge waves (lines) forming at specified anatomical locations (thin black arrows). Thick arrows mark directions of wave propagation.

(F) Illustration of digit patterning (right) and underlying R-D signaling network (left). SOX9-expressing cartilage digit primordia (oval structures) are specified by long-range BMP signaling (green) from interdigit mesenchyme, while inhibition of chondrogenic fate in the latter is driven by short-range acting WNT signaling (blue).

(G) Illustration of digit pattern phenotypes upon WNT inhibition—digit fusion (middle) and BMP inhibition—loss of digits (right).

(H) Illustration of digit pattern phenotypes in *Gli3* and *Gli3/Hoxd11-13//Hoxa13* mutants. Digits are marked with orange and their number are indicated. Red lines mark corresponding digit wavelength.

depend on and affect the signaling pattern—as the crown enlarges, so does the distance between enamel knots and, thus, the distribution of activators and inhibitors.[47] Intriguingly, analogous four-cusped upper molars have convergently evolved numerous times in placental mammals from an ancestral tri-cusped molar.[48] Modeling predicts that ancestral tri-cusped molars can produce four-cusped molars with only a small increase in the activator coupled with posteriorly biased crown growth—this enables the emergence of the fourth knot and rearrangement of all knots into a rectangular pattern.[49] Thus, precise the number and arrangement of patterned elements can be achieved by mild modulations in Turing-model parameters coupled with uneven growth of the patterning field. Collectively, the previously discussed examples underscore the pervasive reliance of embryonic morphogenesis on self-organized molecular patterning. Studying morphogenesis provides insights into gene regulatory modules and signaling pathways commonly used to implement Turing-like patterns, and this knowledge can be readily applied to patterns in adult tissues, which remain mechanistically understudied.

FUNCTIONAL PATTERNS IN ADULT TISSUES

Patterns are ubiquitous in healthy adult tissues and also form *de novo* upon physiological responses and in disease. While adult tissues usually display stable morphological periodicity established during their embryonic morphogenesis—for example, scalp skin features a whorl of clockwise-oriented hairs—in other scenarios, they undergo dynamic remodeling with features of periodic self-organization. Subsequently, we discuss known examples of such pattern-forming physiology.

Tissue waves

Numerous organs contain tissue elements capable of cycling, and their physiology oftentimes depends on coordinated cycling of all such elements. In the heart, cardiomyocytes undergo action potential cycles, wherein voltage across their plasma membrane briefly changes and is mediated by differential ion flow. They also transfer action potentials to their neighbors via gap junctions, resulting in large-scale electrical coupling. Furthermore, specialized pacemaker cardiomyocytes, which have an inherently faster action potential, reside within defined locations of the heart. They ensure that electrical waves regulating whole-heart contraction propagate in a manner that allows atrial contraction before ventricular contraction, which, in turn, precedes whole-heart relaxation. This example illustrates how physiological activity waves can self-organize across tissues (1) if individual tissue elements repetitively cycle and (2) couple with neighboring elements and (3) if such cycles include a refractory phase that blocks coupling. These requirements can be reproduced by a cellular automaton model which describes spatially distributed self-organized processes occurring in a coupled grid of simulated cells. Each such cell cycles through a set of consecutive states, with the decision to remain in the same state or to transition to the next, being influenced by the summation of neighboring cell states on a grid.[50]

Could analogous wave-like phenomena self-organize in non-electrically coupled tissues and instead be mediated by soluble growth factors? Intriguingly, many mammals grow their fur in waves which periodically propagate across the entire skin (Figures 4A and 4B).[51] The building blocks of such waves are cycling hair follicles. The onset of a new hair growth cycle is marked by proliferative activation of dormant (telogen) follicles. Such dormant follicles are otherwise diminutive in shape and principally consist of non-dividing stem cells which closely associate with specialized dermal papilla fibroblasts whose secreted factors promote stem cell quiescence. Upon transition to active growth (anagen), dividing hair stem cells generate hair matrix progeny that, in turn, generate hair fibers—an intricate process supported by dermal papilla fibroblasts that "replace" their original pro-quiescence signals with new pro-growth signals. After some time, which varies across species and body sites, anagen follicles undergo apoptotic regression (catagen), stop growing hair, and remodel back to their dormant state, completing the cycle (Figure 4A).

Intriguingly, telogen timing in individual follicles is remarkably malleable and is influenced by the growth status of neighboring follicles. Anagen follicles potently stimulate new growth of their telogen neighbors, a phenomenon perceivable as macroscopic hair-growth waves (Figure 4C). In animals with pigmented fur, such waves can be easily observed upon periodic fur clipping: shaved telogen skin appears pink and anagen skin is black, while waves appear as gray gradations.[51] At the wave "crest," WNT signaling in telogen dermal papilla cells, likely driven by anagen neighbor-secreted WNT ligands and agonists,[52] heralds follicle activation.[53] WNT factors expressed by anagen follicles are meant to promote their own hair fiber growth, but since follicles are not molecularly insulated and exist at sub-millimeter distances from one another, paracrine factors effectively diffuse and trigger signaling in neighboring follicles. Upon WNT activation, telogen dermal papilla cells produce additional signals, including TGFβ, SCUBE, and FGF ligands and BMP antagonists, that collectively activate hair stem cells, driving new anagen entry (Figure 4D).

In addition to wave-like anagen propagation, two additional phenomena sustain skin-wide hair growth: telogen refractivity and spontaneous initiation. First, early-stage telogen follicles that remained dormant for less than one month are refractory to WNT signals emanating at the hair-growth wavefront. As a result, hair-growth waves stall, and sharp anagen-telogen boundaries form.[53] Refractivity is caused by quiescence-inducing BMP ligands, abundant in early-stage telogen skin, rather than by inherent hair stem cell incompetence for proliferative activation.[54] Refractivity assures unidirectional propagation of hair-growth waves and prevents unnecessary excessive growth by follicles, an energy-demanding process. Second, spontaneous initiation describes the ability of late-stage (competent) telogen follicles for self-activation, which produces anagen "seed" sites from which hair-growth waves then spread. In mice, spontaneous initiation occurs with low probability, requiring simultaneous WNT activation by at least five neighboring telogen follicles.[53] Physiologically, only approximately 5% of dermal papillae become stochastically WNT active within competent telogen skin, most of them solitarily (Figure 4E). Only in rare instances do five WNT-active dermal papillae occupy a similar neighborhood, such that their secondary activators can reach

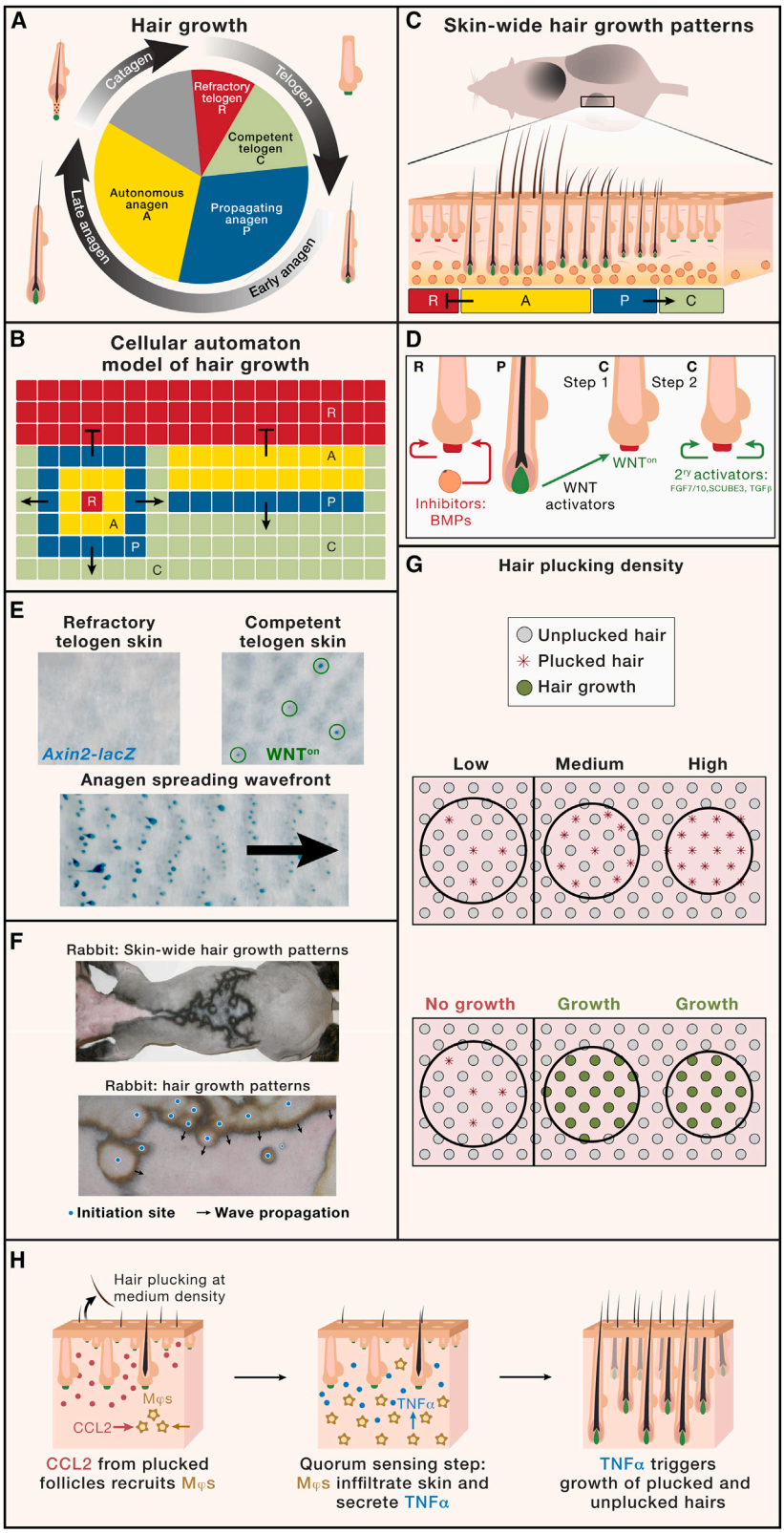

Figure 4. Renewal and regeneration patterns in adult tissues

(A) Illustration of the hair-growth cycle. Cycle phases are indicated along the outer circle in a clockwise direction. Corresponding hair-follicle morphologies are shown outside the circle. Color-coded segments within the circle mark functionally distinct hair cycle states, essential for collective hair growth.

(B) A cellular automaton-like model for collective hair growth. The hair-follicle array is shown as a two-dimensional grid, with squares representing individual follicles. Functionally distinct follicle states are color coded according to A. Interaction rules between follicle states are annotated.

(C) Illustration of skin-wide hair growth waves in shaved pigmented mice (top). Pink—telogen skin, gray shades—anagen skin. Section across skin with hair growth wave is illustrated at the bottom.

(D) Illustration of signaling events in the refractory skin (left) and at the wavefront between signal emitting anagen follicle (center) and signal-receiving telogen follicles (right). Signals are indicated.

(E) Wholemount β-Galactosidase staining of *Axin2-lacZ* WNT reporter skin. LacZ^{+} dermal papillae (blue) are circled green.

(F) Skin-wide hair growth waves in rabbits.

(G) Illustration of quantitative hair-plucking experiment. Top illustrates alternative hair plucking densities, bottom illustrates resulting hair growth responses. Telogen follicles are marked gray, plucked telogen follicles are marked with red asterisks, anagen follicles are marked green.

(H) Illustration of the plucking-stimulated hair-growth response mechanism. Key cellular players and signals are color coded.

the necessary threshold for stem cell activation. Thus, even highly complex physiological processes, such as hair growth, can self-organize into dynamic patterns as long as repetitive tissue elements adapt the same minimum set of rules (Figure 4B).[55] Intriguingly, the same rules that manage fur renewal in mice also operate in much larger animals, such as rabbits, producing visually captivating hair-growth fractal patterns (Figure 4F).[53]

Tissues with cellular automaton-like behavior can rapidly diversify their pattern-forming behaviors without having to fundamentally alter their organization. Indeed, derived hair-growth behaviors are common. Compared to adult mice, fur renewal in aged mice is characterized by slow-moving and fragmented waves, caused in part by decreased expression of follistatin, a BMP antagonist, within competent telogen skin. This likely hinders hair-to-hair coupling, making wave spreading inefficient.[56] In contrast, skin of young mice features fast-sweeping hair-growth waves with conspicuous bilateral symmetry that depends on inherently high spontaneous anagen initiating potential of ventral hair follicles. Indeed, anagen seed sites in young mice first form in the ventral skin from where hair growth waves naturally propagate over the body's flanks onto the dorsum, creating the perception of bilateral patterns.[57] Ventral and dorsal skin differentially express numerous paracrine factors, with the former being enriched for hair-growth activators. Intriguingly, grafting ventral skin onto the dorsum produces a kind of hair-growth pacemaker. Hair growth in ear skin is particularly slow, with local follicles becoming "locked" in a protracted telogen, not responding to hair-growth waves constantly incoming from the nearby head and neck skin. Such hyper-refractivity by ear follicles is non-autonomous and is caused by high levels of BMP ligands and WNT inhibitors expressed in adjacent ear cartilage, and it can be rescued in transgenic mice overexpressing either the BMP antagonist Noggin or WNT ligand, where many more ear follicles spontaneously re-enter anagen.[57] Thus, vastly different tissue-renewal dynamics can self-organize in response to globally changing activator and/or inhibitor levels that in turn alter signaling thresholds for successful coupling between cycling tissue elements.

Injury sensing

Patterned adult tissues rely on their self-organizing properties to effectively sense and respond to supra-physiological stimuli, such as external injury. Animals constantly lose hair by normal "wear-and-tear," such as when grooming, which does not significantly compromise the overall fur density. Yet, if a clump of hair gets pulled, such as upon fighting, the resulting denuded skin would necessitate local hair regrowth ahead of normal schedule. Indeed, experimentally, controlled plucking of one to twenty hairs in mice is "ignored," while plucking of over fifty adjacent hairs rapidly triggers new anagen.[54] How does skin measure the extent of hair loss? The underlying mechanism must involve "follicle counting" and density-dependent decision making, a form of quorum sensing. Supporting this possibility are the results of hair plucking at decreasing densities—when the same number of hairs are plucked sparsely, new hair growth is triggered only above certain density. Intriguingly, at such threshold density, all follicles within the area—both the plucked ones and all of their un-plucked neighbors—reenter new growth, producing an amplifying effect (Figure 4G).[58] Because, at threshold density, plucked follicles are approximately a millimeter apart, and this far exceeds physical distances at which paracrine signals can effectively function. Thus, short-range signals secreted by plucked follicles need to be somehow extended over space and then accessed by all follicles in the region. This is accomplished via two signals and signal-amplifying cellular vectors: (1) plucked follicles secrete the first signal, chemokine CCL2, (2) macrophages respond to CCL2 and swarm into plucked skin in proportionate to the density of plucked hairs, and (3) macrophages secrete a second signal, TNFα, which (4) acts on hair stem cells, stimulating anagen entry by all follicles regardless of their plucked status (Figure 4H).[58] Size-threshold sensing upon hair plucking appears to be analogous to wound-size sensing (Figure 2C), whereas new hair formation is triggered only in wounds that are too large to be efficiently covered by pre-existing peri-wound hairs.

This example also illustrates how migratory cells can bridge molecular communication between distant tissue units. Owing to their effectiveness, adult tissues rely on migratory immune cells to "quantify" injury in diverse contexts, and many non-immune tissue cells are inherently responsive to pro-inflammatory cytokines, chemokines, and interleukins. Immune-mediated injury sensing plays a particularly vital role upon wounding, helping tissues to launch distinct repair mechanisms commensurate to minor, moderate, or major damage. At the same time, diseases with pattern-forming features can arise from excessive immune-cell recruitment and/or pathologically heightened sensitivity to inflammatory signals.

De novo patterns

Regeneration is a profound injury-response mechanism, wherein embryonic-like processes reactivate locally to reform complex, and oftentimes patterned, tissue elements. How do adult tissues deploy pattern formation for regeneration, and to what extent do underlying mechanisms of regeneration differ from highly efficient processes that drive fetal tissue morphogenesis? Animals such as house mice, acomys (African spiny mice), and rabbits heal large skin wounds with new hair-bearing tissue via a regenerative processes called hair neogenesis. Morphologically, hair neogenesis replicates embryonic hair formation—first, individual epithelial placodes form, then mesenchymal condensates form underneath them, and such primordia go on to mature toward fully functional follicles.[20] Intriguingly, hair neogenesis in house mice is limited to the wound center, while in acomys it occurs across their entire wound, first starting at the periphery and then propagating toward the wound center,[59] suggesting that analogous to embryonic patterning, regenerative patterning can be constrained by initial conditions—wound-edge incompetence in house mice and early wound-edge competence in acomys.

What underlies regenerative competence in skin wounds? Analogous to embryonic hair formation, hair neogenesis depends on WNT signaling. Indeed, overexpression of WNT antagonist *Dkk1* in mice completely blocks hair neogenesis, while *Wnt7a* overexpression produces supernumerary follicles, yet only in the wound center.[20] In contrast, transgenic activation of SHH signaling in wound fibroblasts results in dense hair

neogenesis across the entire wound bed.[60] This suggests that the initial condition constraining regeneration likely comes in the form of epigenetic competence of wound fibroblasts rather than pattern-driving WNT factor availability. Curiously, follicles regenerate in wound regions that display a narrow range of biomechanical tissue stiffness, between 5 and 15 kPa. In acomys, such permissive stiffness values are exhibited across the entire wound but at the periphery first, while in house mouse, stiffness at wound periphery never drops below 20 kPa.[59] Thus, for skin wounds to display competence for *de novo* pattern formation, certain epigenetic cell states need to be surrounded by a specific biomechanical and signaling tissue-level environment.

What influences how many hairs regenerate within competent parts of the wound? Unlike highly efficient embryonic hair development, hair neogenesis is strikingly variable from mouse to mouse, producing from as few as one to many hundreds of follicles. As discussed previously, embryonic hair formation occurs in consecutive waves, with later-born follicles forming in large numbers at WNT symmetry-breaking points around earlier-born follicles as skin expands around them. Hair neogenesis cannot replicate this high-efficiency process because wounds do not expand in size after their initial closure. Moreover, the cellular milieu of wounds is highly heterogeneous and enriched for immune cells that both secrete paracrine factors and actively migrate, making their signaling contributions noisy. Yet, immune cells significantly impact hair neogenesis. Specifically, γδ T-cells migrate into wounds ahead of hair regeneration and secrete FGF9, which triggers WNT ligand expression in fibroblasts.[61] This immune contribution is significant since mice deficient for γδ T-cells, or with T-cell-specific *Fgf9* deletion, regenerate fewer hairs than wild-type mice. Innate immune cells also regulate hair neogenesis and, for example, increased numbers of phagocytic macrophages correlate with loss of neogenesis.[62] Paradoxically, wounds enriched for phagocytic macrophages also display high WNT signaling which, when aberrantly activated, can drive fibroblasts toward scar-making states. Mechanistically, high WNT signaling arises from unrestrained phagocytosis of fibronectin-bound WNT antagonist SFRP2. Indeed, wounds in mice with reduced macrophage numbers, or with inhibited phagocytosis, heal with increased hair neogenesis efficiency.[62] Thus, regenerative patterning has low efficiency because of sub-optimal spatial constraints, cellular players, and dual-purpose signaling.

SELF-ORGANIZED PATTERNS IN DISEASE

Thus far, it appears that self-organizing processes commonly drive stable morphological patterns in embryonic tissues and transient patterns in adult tissues. What actually becomes self-organized in space is usually the molecular information, which then instructs spatially distributed cell behaviors like proliferation, apoptosis, migration, etc. When we observe striking periodic patterns, we are looking at the final outcome of a pattern implementation process, a morphological "afterglow" of the initial molecular self-organization. Thus, a morphological pattern informs that a tissue engaged in self-organization at crucial stages of its development or physiology.

By analogy, if a disease features a morphological pattern, it means that the diseased state is accompanied either by aberrant molecular self-organization and/or aberrant implementation of patterned information. Differential diagnosis of many diseases, especially in pathology and dermatology, is rooted in morphological discrimination of spatial patterns. Yet, while medical professionals rely on pattern recognition for diagnosis, studies of disease mechanisms do not usually consider such patterns, as they focus on identifying disease-driving molecules and cell types but typically not their periodic distribution. Developmental biology teaches us that the most striking phenotypes, like the complete suppression of a pattern, can be achieved by perturbing pathways involved in molecular self-organization rather than pathways part of downstream implementation processes. For instance, complete suppression of digit formation occurs upon inhibition of the BMP pathway, an activator in a Turing-like circuit for digit specification (Figure 3G),[43] while deletions of genes involved in skeletal outgrowth, such as *Wnt5*a or *Vangl2*, result in shorter digits, but not their loss.[63] Hereafter, we propose that identifying and interfering with signals and cell types that initiate pattern formation can become an efficient future strategy for disease therapy. At present, however, our understanding of pathological patterns remains largely rudimentary. Next, we highlight selected examples of such patterns and discuss known pattern-driving factors.

Skin disease waves

Dermatological diseases commonly display primary lesions, like fluid-filled vesicles and pustules, or differentially colored macules and patches. Sometimes lesions are solitary, yet oftentimes they are numerous and dynamic, propagating across the skin as "pathological waves." For example, striking wave-like patterns arise upon erythema gyratum repens—red and scaly skin self-organizes into target-like rings and self-warping spirals across a patient's trunk (Figure 5A).[64] While disease pathogenesis remains unclear because it commonly accompanies underlying malignancies, it is hypothesized to represent a patterned immune response to endogenous skin antigens being mimicked by distant tumor neo-antigens.[65]

Regardless of etiology, pattern-forming skin diseases behave analogously to a hair-growth wave even though their cellular and signaling components are likely distinct from those involved in hair-cycle regulation. Principally, wave behavior by a given skin disease would, at a minimum, require cutaneous tissue micro-domains to exist in at least three mutually exclusive states: (1) physiological state, (2) active disease state, and (3) chronic or post-disease state. Secondly, in their active disease state, one or several micro-domain cell types should produce signals to which adjacent, unaffected micro-domains respond by entering an active disease state. In this way, a pathological wave can propagate into unaffected skin, enlarging lesions. Moreover, in a chronic or post-disease state, the same cell types should be refractory to the same signals, preventing retrograde wave propagation. Within this framework, a range of disease patterns is possible. For example, if tissue micro-domains quickly transition from active to post-disease and then back to normal state, such recovered micro-domains can become re-engaged, and disease waves emerge in the form of multiple concentric circles

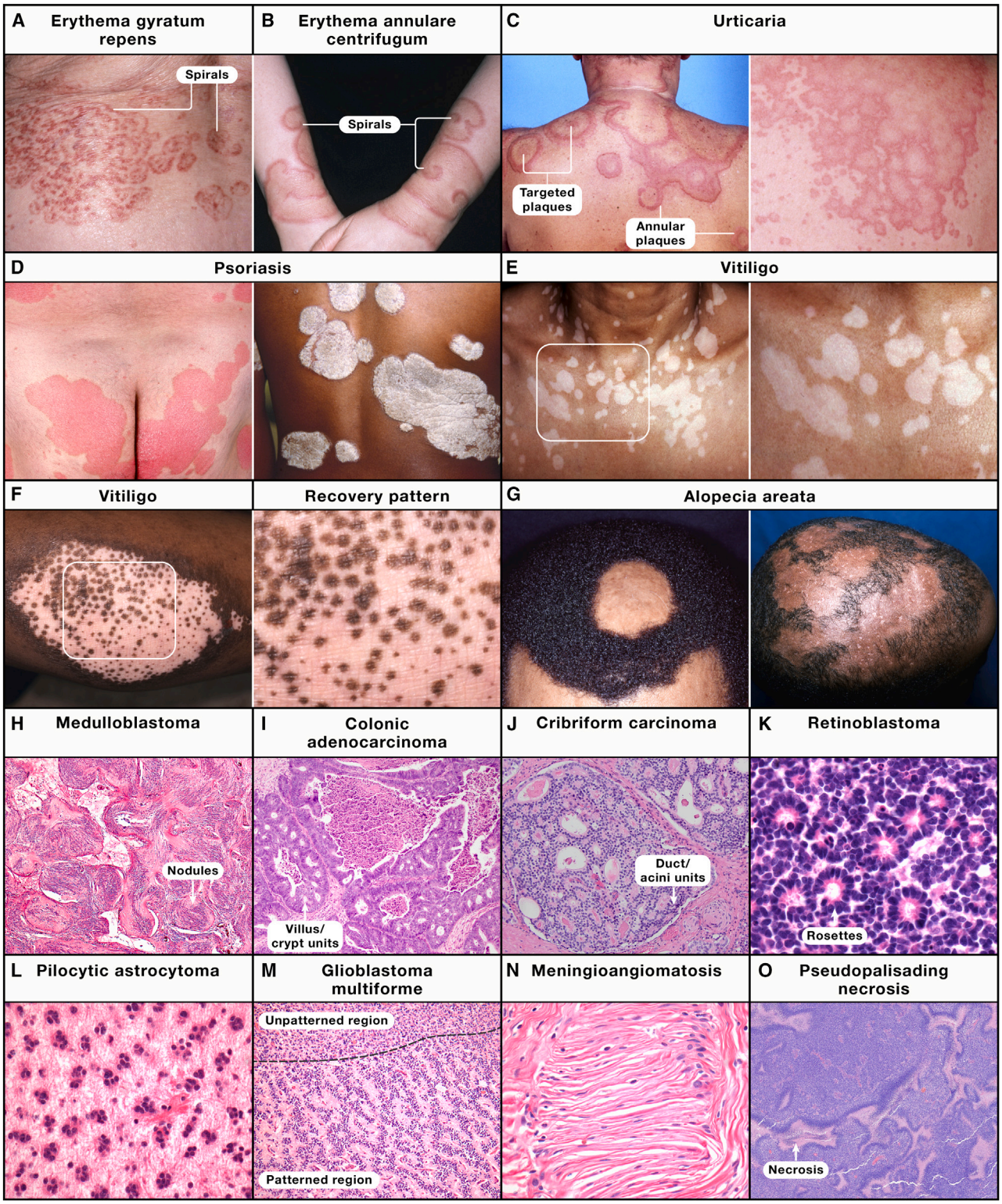

Figure 5. Skin diseases with prominent patterns

(A) Erythema gyratum repens on the chest skin. Spiral-shaped patterns are marked.

(B) Erythema annulare centrifugum on the forearm skin. Spiral-shaped patterns are marked.

(C) Urticaria on the upper trunk skin. Left shows drug-induced urticaria multiforme with edematous, erythematous annular, and targetoid plaques (marked). Right shows urticaria with multiple coalescing edematous papules with lighter centers.

(legend continued on next page)

or self-warping spirals (Figures 5B and 5C). If a disease has high initiation rate, then numerous pathological waves from adjacent primary lesions could merge into complex fractal shapes.

Psoriasis

Psoriasis is a chronic auto-inflammatory skin disease. Its common form, plaque-type psoriasis, features persistent red and scaly lesions. Lesional epidermis is thickened and incompletely differentiated and overlays dense immune cell infiltrates. New lesions start as drop-like sites that expand centrifugally and coalesce into larger plaques with complex wavefronts (Figure 5D). Importantly, molecular interactions between keratinocytes and dendritic and T-cells at such wavefronts produce pathological signals that facilitate disease spreading into unaffected skin.

An essential early pathogenic event in psoriasis is aberrant activation of the so-called plasmacytoid dendritic cells. They become stimulated by a number of the so-called stress molecules—self-DNA, cytokines, and antimicrobial peptides—secreted by skin keratinocytes. Activated plasmacytoid cells initiate a cellular chain reaction which culminates with the activation of T-cells by locally produced diffusible cytokines, such as TNFα, IL-12, and IL-23.[66] Among these cytokines, IL-23 and its target Th17 T cells are thought to be particularly indispensable for psoriasis pathogenesis. Th17 T cells migrate in large numbers into the affected skin, where they recognize and signal to stressed keratinocytes via cytokine IL-17,[67] inducing them to expand and aberrantly differentiate into clones of disease-sustaining cells. At the end of this pathogenic pathway, the skin affected by psoriasis chronically remodels its immune-cell composition, immune-keratinocyte signaling crosstalk, and epidermal differentiation program. Importantly, diffusion of stress molecules from keratinocytes beyond the edges of psoriatic lesion results in pathogenic immune cell clusters and associated cytokine networks assembling within the adjacent unaffected skin, enabling for the disease-causing wave to advance. Intriguingly, psoriatic skin patterns can be faithfully simulated with a mathematical model that considers (1) a minimal, biologically educated set of secreted cytokines that stimulate Th17 T-cells and (2) the initial state of randomly seeded clusters of Th17 T-cells.[68] Simulations using this model predict that disrupting one of two essential cytokines, IL-17 or IL-23, can be sufficient to stall disease-driving clustering of Th17 T-cells. Indeed, neutralizing antibodies against IL-17[69] and IL-23[70] are clinically effective at clearing psoriatic plaques and preventing disease progression.

Vitiligo

Vitiligo is an autoimmune disease manifested as patterns of skin depigmentation. Analogous to psoriatic plaque patterns, vitiligo patches display centrifugal growth and fusion into complex fractals (Figure 5E). Normally, melanocytes reside in the basal epidermal layer, where they transfer organelles called melanosomes to adjacent keratinocytes, endowing epidermis with pigment. Long-lasting epidermal depigmentation in vitiligo results from $CD8^+$ T-cell-induced death of melanocytes at the disease wavefronts.[71] Factors, including reactive oxygen species, trigger melanocytes to secrete damage-associated molecular patterns (DAMPs), such as auto-antigens and heat shock proteins. Dendritic cells recognize DAMPs and present them to T cells, stimulating auto-reactive $CD8^+$ T cells. Dendritic cells also secrete interferon-γ, which signals to keratinocytes via the JAK/STAT pathway, inducing chemokine production.[72] Key in this cascade are CXCL-9 and CXCL-10, which recruit auto-reactive $CD8^+$ T cells toward the epidermis, where they both (1) amplify interferon-γ signaling, thereby producing sustained pathogenic cellular collectives and (2) target melanocytes for apoptosis in an autoimmune attack, producing a depigmentation effect.[73] Importantly, analogous to psoriasis, diffusion of interferon-γ and chemokines at the vitiligo wavefront results in pathogenic cellular collectives consisting of stressed keratinocytes and $CD8^+$ T cells assembling within the adjacent skin, forming the basis for the sustained propagation of melanocyte-killing autoimmune wave. Given this mechanism, disrupting interferon-γ and/or chemokine signaling could efficiently halt depigmentation wave spreading. Indeed, JAK inhibitors, which disrupt the interferon-γ-induced JAK/STAT pathway, are therapeutically effective for vitiligo, and topical JAK1/2 inhibitor Ruxolitinib has been approved by the U.S.A. Food and Drug Aministration (FDA) for treatment of acquired vitiligo.[74] Moreover, mice that received adoptive transfer of premelanosome protein-specific $CD8^+$ T cells and developed a vitiligo-like phenotype experienced reduced tail-skin depigmentation following treatment with CXCL10-neutralizing antibody.[73]

While some vitiligo cases feature chronic disease state and persistent depigmentation,[75] in other cases, such as in patients receiving JAK inhibitors, a post-disease state develops, when intact melanocyte stem cells residing in hair follicles stably migrate out into the adjacent epidermis, driving its repigmentation. This produces vitiligo recovery patterns that follow natural hair-follicle distribution patterns and present as matching patterns of circular,

(D) Psoriasis on the trunk skin. Left shows numerous well-demarcated, salmon-pink psoriatic plaques. Right shows large, confluent, well-demarcated plaques with overlying thick white scales.
(E) Vitiligo showing multiple depigmented macules and patches on the neck and chest.
(F) Vitiligo showing depigmented patch with areas of repigmentation (magnified).
(G) Alopecia areata with single (left) and multiple (right) hair-loss patches.
(H–K) Tumors with high redifferentiation potential and self-organized patterning: medulloblastoma (desmoplastic/nodular variant) with cerebellar cortical-like patterns (H), colonic adenocarcinoma with repetitive villus/crypt-like patterns (I), prostatic cribriform carcinoma with repetitive glandular duct/acini-like patterns (J), and retinoblastoma with repetitive neural rosettes (K).
(L) Pilocytic astrocytoma with periodic pattern of spot-like cell clusters.
(M and N) Glioblastoma multiforme (M) and meningioangiomatosis (N) with periodic cell arrangements.
(O) Pattern-forming pseudopalisading necrosis in glioblastoma.
Images for this figure we kindly provided with the following permissions: 5A, 5B, 5C, (right), and 5G (left) by Jeffrey Callen; 5H and 5K–5N by Edwin Monuki; 5I by Vishal Chandan; 5J by Giovanna Giannico; and 5O by Mari Perez-Rosendahl. Images in 5A–5G were used with permission from VisualDx. 1A–1C and 1E–1G were from iStock and 1H–1I from Shutterstock (under standard license). Additionally, we thank Ashley Gamayo, Cary Johnson, Sherif Rezk, Sejal Shah, Beverly Wang, and William Yong for providing pathology images used in Figure 5.

pigmented micro-patches that expand centrifugally from follicular openings (Figure 5F).

Alopecia areata

Similar to vitiligo, alopecia areata is an autoimmune skin disease with shared cellular players (i.e., $CD8^+$ T cells), signaling mediators (i.e., interferon-γ), and efficacious therapeutics (i.e., JAK inhibitors). Alopecia areata manifests as expanding patches of hair loss that are most obvious on the scalp (Figure 5G). Disease targets hair matrix cells at the base of growing follicles.[76] Normally, human scalp follicles continuously grow for multiple years, and matrix cells experience relative immune privilege, with low expression of major histocompatibility complex (MHC) class I and II molecules.[77] However, certain triggers such as viral infection and associated cytokine storm in genetically predisposed individuals can upregulate MHCs in matrix cells, resulting in their immune-privilege collapse and cytotoxic attack by $CD8^+$ $NKG2D^+$ T cells primed against certain hair auto-antigens. As in vitiligo, $CD8^+$ T cells secrete interferon-γ, activating the JAK/STAT pathway in hair-matrix cells which, in turn, secrete numerous cytokines and, principally, IL-15. The latter reciprocally signals to $CD8^+$ $NKG2D^+$ T cells, sustaining their peri-follicular swarming and continuing cytotoxic attack.[78] Attack on matrix cells disrupts the hair-making process, to which follicles respond by prematurely aborting their growth and shedding hair fibers at the disease wavefront. Affected follicles behind the wavefront fail to produce long hair, despite attempting to restart growth, due to incessant growth-terminating autoimmune attack.[76]

Alopecia areata is intriguing from the patterning perspective. Its tissue micro-domains—individual hair follicles—are spaced apart by fairly large distances measuring around 1–1.4 mm.[19] Yet, despite these distances exceeding typical signaling-factor diffusion lengthscales, propagation of the autoimmune attack across follicle population is efficient. This suggests the existence of an as-yet-unknown long-range bridging mechanism. It is plausible, however, that similarly to macrophage swarm-mediated hair growth after plucking in mice,[58] hair-to-hair alopecia areata propagation in humans relies on "imperfect" $CD8^+$ T cell swarming, such that sufficient numbers of immunocytes migrate "off-target" toward unaffected follicles to generate pathogenic interferon-γ signaling.

The aforementioned examples illustrate how diseases that clinically present with morphological patterns rely on aberrant self-organization of pathogenic cell clusters involving at least (1) one stationary cell type (e.g., keratinocytes), (2) one migratory immune cell type (e.g., T cells), and (3) one pair of paracrine signals coupling them together. Diffusion of signals and immune-cell swarming toward these signals generate "imperfect" pathogenic cell clusters and their wave-like "spillage" into healthy adjacent tissue. Not surprisingly, pharmacological disruption of pattern-driving signaling pathways offers effective therapy for such diseases.

Pathological patterns in cancers

Similar to skin diseases, cancers are rife with periodic patterns. As cancers are new growths (neoplasms), patterning may provide them with some of the same advantages enjoyed by developing embryonic tissues: (1) enabling rapid growth of heterogeneous cell clones, (2) supporting co-existence of functionally sub-specialized tissue domains, and (3) increasing robustness in the face of natural defenses, including the immune system. Patterns are also central to cancer classification. Repetitive microscopic features, referred to as "architectural patterns" by pathologists, split dividing cancers into subtypes, inform cancer prognosis and therapeutic strategies, and train machine learning algorithms for automated cancer recognition.

Insofar as pattern-forming mechanisms may enable tumors to grow optimally, they can suggest novel therapeutic targets. Cancers prototypically start as mutated cell clones with enhanced proliferation, self-renewal, and/or survival characteristics and, eventually, spread via local invasion and long-range metastasis. Mutated oncogenes and tumor-suppressor genes typically drive carcinogenesis and, along with other "passenger" mutations, assemble new, pathological gene-regulatory networks that endow cancer cells with growth advantages. Cancer-initiating cells also commonly undergo "dedifferentiation" toward developmentally earlier progenitor-like states, a feature that has led to their characterization as cancer stem cells.[79] As cancer progenitor cells divide, their progeny "redifferentiate" by recapitulating parts of the developmental program of the tissue of origin, which can conceivably include self-organized patterning, albeit with notable changes—tumor patterns are often noisy, with aberrantly frequent and morphologically imprecise periodic elements. One such tumor is the mature ovarian teratoma, which arises from post-meiosis I germ cells and features tissue derivatives of all germ layers, some of which become highly patterned, such as hair follicles or teeth.[80] Analogously, common childhood brain neoplasms, called medulloblastomas, arise from cerebellar stem cells harboring differentiation-preventing mutations[81] and histologically recapitulate patterned features of cerebellar cortical morphogenesis, albeit with high stochasticity and unnatural spatial coordinates (Figure 5H). Other prominent examples include colonic adenocarcinoma with repetitive villus/crypt-like patterns (Figure 5I), prostatic cribriform carcinoma with repetitive glandular duct/acini-like patterns (Figure 5J), and retinoblastoma with repetitive neural rosettes (Figure 5K). Dedifferentiation followed by redifferentiation of cancer progenitor cells using pathological gene regulatory networks likely explains why cancer architectures both resemble yet differ from their tissues of origin. Propensity of tumors to self-organize into aberrant patterns can persist upon their metastasis and even *in vitro*, when cancer-initiating cells are grown in monolayer cultures or as organoids.[82]

As cancers progress and genetically evolve, their architectures resemble tissues of origin less and less. Early on, however, pre-malignant, dysplastic lesions often strongly resemble their normal counterparts. Even though progression toward high-grade cancer is typically accompanied by more frequent "poorly differentiated" cells, vestiges of pattern tend to persist. For example, in poorly differentiated adenocarcinomas, cells no longer form glands but continue to grow as clusters, indicating preservation of homotypic cell-cell adhesion despite the loss of glandular morphogenesis pathways. Periodic patterns in normal tissues are typically preceded and instructed by self-organizing molecular patterns (Figure 3). At present, molecular understanding of self-organization in cancer is scarce.

Presumably, at least some cancer patterns are underpinned by R-D networks "borrowed" from the tissues of origin. Indeed, signaling pathways implicated in developmental R-D scenarios—WNT, SHH, BMP, and FGF—take part in cancer induction and progression. Thus, it is conceivable that analogous molecular patterning mechanisms underlie at least certain cancers. In this context, cancers with periodic stripes and spots, such as pilocytic astrocytoma (Figure 5L), glioblastoma multiforme (Figure 5M), or meningioangiomatosis (Figure 5N), are especially intriguing. Glioblastomas are commonly associated with epigenetic silencing of soluble WNT antagonists from SFRP and DKK gene families, whose promoters become hypermethylated.[83] Speculatively, such epigenetic changes can drive nuanced rather than "all out" WNT activation, which can, conceivably, enable it to enter a pathological pattern-forming regime.

Still, despite tantalizing correlations, cancer biology at present lacks systematic insight into molecular mechanisms that underlie periodic neoplastic tissue growth. In fact, what pathologists perceive as cancer patterns may arise through non-R-D mechanisms, for example, through preferential expansion of cancer cells along vascular network set up by angiogenesis. In this regard, the effects of cancer-associated fibroblasts, immune cells, and other cell types on patterned tumor growth are equally obscure. Yet, *de novo* tumor patterns can arise in cooperation with non-autonomous cell events, such as within glioblastoma around clusters of necrotic cells, so-called pseudopalisading necrosis (Figure 5O). We anticipate that future research on this topic will yield new insights into cancer pathogenesis and that it might inspire a search for unconventional cellular and/or molecular therapeutic targets.

PATTERN ENGINEERING WITH SYNTHETIC BIOLOGY

In vivo examples of pattern formation highlight that self-organizing mechanisms based on genetically encoded intercellular communication networks are intertwined with upstream initial conditions of morphogenetic fields and downstream pattern implementation mechanisms. Intriguingly, *in vitro* systems also display pattern formation. For instance, pluripotent stem cells (PSCs) and adult stem cells can develop into patterned organoids under the right culture circumstances, offering *ex vivo* platforms for studying self-organization.[84] Examples include organoids with repeated somitic structures (Figure 6A), cerebral organoids with neural rosettes (Figure 6B), skin organoids with hair follicles (Figure 6C), and intestinal organoids with alternating crypts and villi (Figure 6D). Unlike *in vivo*, self-organization in organoids starts from a disorganized initial state, often a cell suspension. Therefore, initial constraints are low or null, and self-organization relies on intrinsic pattern-forming ability of cells. Lack of initial constraints also underlies variability in the resulting structures. Yet, this can be considered a perfect opportunity to identify constraints that could increase patterning robustness and improve our understanding of self-organizing mechanisms. Nonetheless, low pattern reproducibility constitutes a hurdle toward organoid use in drug screening and regenerative medicine. Thus, next-generation organoid technologies incorporate additional control mechanisms, provided by microfluidic devices, advanced biomaterials, three-dimensional (3D) printing technologies,[85] etc. However, deeper understanding of pattern formation mechanisms *in vitro* is required to fulfill the potential of these technologies, including *ex vivo* production of patterned tissues for transplantation.

To this end, one experimental strategy consists of constructing artificial patterning events through the introduction of genetic circuits designed to control cell communication and signal processing. These synthetic biology approaches were pioneered in bacteria, where genetically encoded signaling networks and morphogen-like signaling sources can induce patterns like bullseyes and stripes.[86] More recently, patterns were engineered in mammalian cells via computationally designed networks and use of natural or synthetic signaling components.[87] In these minimalistic settings, pattern-formation details can be better elucidated and further engineered in isolation from confounding factors. With advances in genetic engineering and synthetic cellular crosstalk, convergence is emerging between synthetic and organoid biology.[88] Synthetic biology tools increasingly enable constraining initial conditions in organoid culture to enhance pattern reproducibility or to complexify their structure.

Patterns in cell culture

R-D patterns can be induced in cultures of epithelial cells using natural diffusible activator Nodal and its repressive binding protein Lefty as an inhibitor (Figure 6E).[89] By engineering cells with a genetic circuit where Nodal-responsive promoter lies upstream of Nodal, Lefty, and a luciferase reporter, Turing-like patterns of luciferase activity spontaneously emerge. Key to this pattern-forming behavior is the short diffusion range of Nodal, caused by its finger-1 domain. Removal of this domain or its addition onto Lefty equilibrates diffusion ranges, abolishing patterns.

Patterning in cell culture can also be engineered with synthetic signaling pathways, which have advantages as (1) they do not interfere with endogenous gene-regulatory networks and (2) their strength and specificity can be adjusted by user-defined genetic modifications. Synthetic tools can enable engineering of initial conditions upon which cells would connect endogenous gene regulatory machinery to, for instance, assemble into stereotypical patterns.[90] One such engineered tool is based on synthetic Notch (synNotch) receptors.[91] SynNotch receptors imitate natural Notch receptors with extracellular domains switched to recognize user-defined ligands and intracellular domains switched to exogenous transcription factors, enabling user-defined orthogonal control of gene expression. Upon Notch-mediated signaling, ligand-receptor binding triggers proteolytic release of receptor's intracellular domain, which translocates to the nucleus to activate gene expression. Although synNotch receptors commonly recognize membrane-bound ligands, they can also recognize soluble factors bound to membrane-tethered anchors.[92] SynNotch receptors engineered to recognize either soluble green fluorescent protein (GFP) or mCherry proteins can induce a synthetic morphogen gradient system responsive to a synthetic ligand. By changing anchor-protein abundance or by adding an opposing inhibitory pole, the gradient's length and shape could be controlled. Moreover, by adding positive feedback loops and mixing two cell types, *in vitro* patterns with

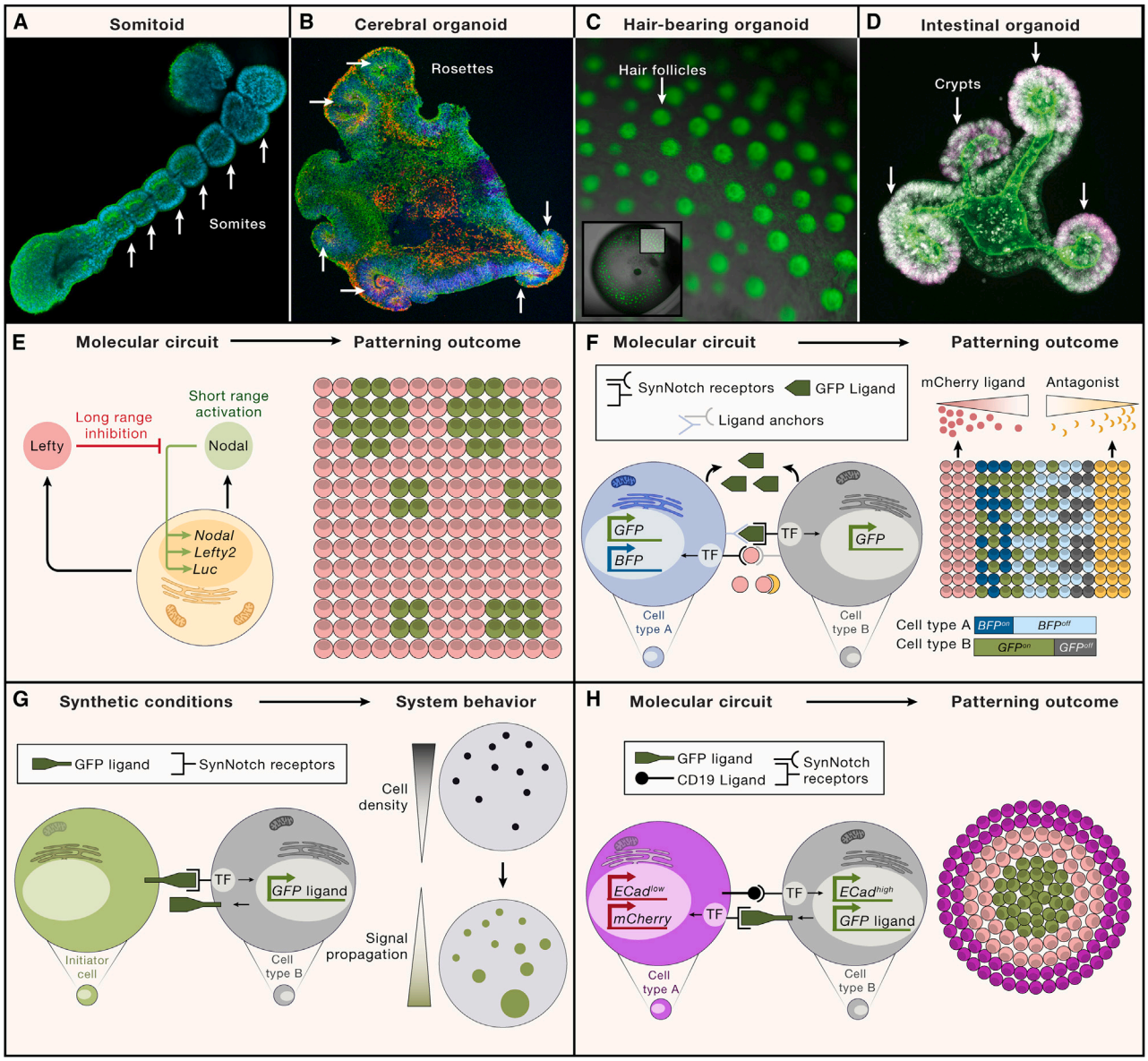

Figure 6. Synthetic biology approaches to patterning *in vitro*

(A) Somitic organoid on day 7 of culture. Individual somites are marked. Green: phalloidin, blue: DAPI.

(B) Cerebral organoid on day 35 of culture. Neural rosettes are marked. Green: *Foxg1-Venus* reporter (forebrain marker), red: Tbr1 (neuronal marker), white: Sox2 (progenitor marker), blue: Hoechst.

(C) Hair-follicle-bearing organoid on day 76 of culture. Individually patterned hair follicles (green) are shown, with the entire organoid shown in the inset. Green: *Desmoplakin-GFP* reporter.

(D) Intestinal organoid on day 4 of culture. Crypt domains are marked. Green: phalloidin, purple: YAP, white: DAPI.

(E) Illustration of an engineered molecular circuit consisting of the short-range ligand Nodal (green), the long-range soluble inhibitor Lefty (red) and Nodal-dependent transcriptional response (left). Right shows the resulting self-assembling pattern of alternating clusters of Nodal^{high} (green) and Lefty^{high} cells (red).

(F) Illustration of a synthetic molecular circuit (left) and the resulting self-assembling French-flag pattern of distinct cellular states (right). Cell type A (teal) and type B (gray) on the left show their molecular interactions mediated by synNotch receptors recognizing soluble GFP (green) and mCherry (red) bound to both synNotch receptor (black) and anchor receptor (gray), as well as by a soluble mCherry antagonist (orange). Transcriptional activation events are shown within nuclei. When provided with opposing gradients of mCherry and its antagonist, mixed type A and B cells self-organize into a French-flag pattern of reporter states (right).

(G) Illustration of a synthetic molecular circuit (left) and its resulting signaling-wave-forming behavior (right). Here, circular signaling waves initiate from sparsely seeded synthetic ligand-presenting "initiator" cells and propagate via cell-cell contact at cell-density-dependent speed.

(H) Illustration of a synthetic molecular circuit with inducible expression of cadherins in cell types A and B (left) and the resulting self-assembling multi-layered sphere pattern (right).

Images for this figure we kindly provided with the following permissions: 6A by Marina Sanaki-Matsumiya and Miki Ebisuya; 6B by Momoko Watanabe; 6C by Anh Phuong Le, Jiyoon Lee, and Karl Koehler; and 6D by Raul Bressan and Kim Jensen.

sharp boundaries, such as "French-flag" patterns (i.e., patterns consisting of three distinct domains of cells with sharp boundaries in between, as if blue, white, and red stripes on a French flag), could emerge (Figure 6F). By introducing positive feedback loops in receiver cells, SynNotch receptors can also support self-propagating signals,[93] as supported by preliminary evidence in naive mouse fibroblasts where circular signal waves emerge when sparse ligand-presenting "initiator" cells are mixed in. This system reveals that cell density affects signal propagation speed. When cells are cultured with density gradient, signal propagation becomes patterned along such cell-density gradients (Figure 6G). These examples illustrate how cell-cell contact-dependent pathways can be engineered to support diverse self-organized patterning events across cultured cell collectives.

Differential cell adhesion commonly mediates patterns *in vivo*. *In vitro*, expression of two different cadherins in cells with low natural adhesion drives the formation of segregated domains through induced homotypic preference. Combining this with synthetic signaling can, in turn, drive 3D self-organization from initially mixed cells (Figure 6H).[94] By combining two distinctly engineered cell types, spheres showing three concentric layers self-organize from a mixed state through synNotch-induced homotypic preference (Figure 6H). Here, both the initial conditions and the patterning mechanism are user defined via engineering cells' communication and downstream adhesivity. Emerging efforts to precisely control organoid formation can take advantage of both engineering processes. Moreover, synthetic genetic circuits, through their isolation and simplicity, permit dissecting minimal requirements for pattern formation in model cell lines.

Enhancing organoid reproducibility

Unlike embryonic tissues, where prior morphogenetic events serve as natural initial conditions, limiting downstream self-organized patterning, *in vitro* organoids can emerge from a range of initial conditions and produce stochastic patterns. Recently, genetic controls have been tested to stereotype PSC-derived organoids. For example, brain organoids can be guided to produce anatomical structures resembling specific brain regions; yet, generating multi-domain cerebral structures remains a challenge. SHH pathway is an essential regulator of developing brain patterning *in vivo*. *In vitro*, an SHH signaling center can be introduced to brain organoids by appending a spheroid of SHH-expressing stem cells.[95] This creates a long-range SHH gradient that, in turn, promotes reproducible pattern of distinct cerebral domains with dorsal-ventral identity, whereas gradient-lacking organoids only develop dorsal identity. This illustrates how a lack of signaling centers limits organoid complexity and how "nudging" them through artificially created centers is sufficient to complexify patterning.

Geometric arrangement can also enhance organoid reproducibility. For example, when cultured as spheroids, human PSCs arrange into epithelial cysts that break symmetry, forming an anterior neural tube and elongating the posterior tail bud. Yet, such organoids form imperfect patterns with ectopic tail buds and branches unless they are additionally micropatterned into close-knit hexagons with inward-facing anterior poles.[96] In this spatial arrangement, WNT inhibitors secreted by anterior cells of all six organoids sum into a radial gradient in the center of the hexagon. In turn, this radial anterior-to-posterior gradient constrains WNT-dependent elongation of the posterior poles, enabling individual organoids with minimal ectopic branches. As a result, axis elongation in organoids arises in a predefined orientation, enabling stereotypical differentiation of somites through traveling FGF signaling waves.[97] This example highlights the importance of defining morphogenetic fields to constrain organoid self-organization. Future refinements to genetically encode control over gradient formation will likely enable sophisticated PSC-derived organoids with stereotypical organization and cell-type composition.

At the same time, recognizing inherent limitations of PSC-derived organoids, the emerging research on the so-called "integrated embryo models" aims to study mechanisms of early organogenesis, including pattern formation of vital early embryo structures, in cocultures of several embryo cell types.[98] Unlike PSC-only organoids that are regarded as "non-integrated embryo models" capable of simulating only parts of development of individual organs (e.g., brain organoids, optic vesicle organoids, etc.), next-generation integrated embryonic models combine PSCs with two other major cell types naturally present within blastocyst-stage embryos—extraembryonic endoderm and trophectoderm. In combination, co-cultures of PSCs with trophectoderm cells readily assemble into blastoids, cavitated cysts that closely resemble natural blastocyst-stage embryos. While varying *in vitro* protocols for blastoid formation have been reported to date, they all result in highly stereotyped morphologies,[99] suggesting that non-PSCs exert essential control over a range of morphogenetic potential of PSCs, "confining" them toward more natural, *in vivo*-like program implementation. Moreover, extended culture of blastoids on 3D extracellular matrices triggers them to undergo early stages of post-implantation morphogenesis, including key embryonic pattern-forming events such as primitive streak specification and initiation of gastrulation.[100] While the ethical status of integrated embryo models should be strongly considered in any future works, given their advanced differentiation features, they will serve as an invaluable model for establishing underlying mechanisms that naturally pattern early post-implantation embryos along their major body axes.

CONCLUSIONS AND PERSPECTIVES

Pattern formation during embryonic development and postnatal tissue physiology share many principles, and several mathematical models have been put forward to explain their formation. These include Turing-type models as well as French-flag models, which describe generation of positional information from a morphogen gradient, and "clock and wavefront" models, which describe consecutive partitioning of tissue into discrete units as the result of oscillating expression of signaling molecules and/or their gradients. While most such models are conceived at a high level of abstraction, the patterns they produce and the insights they provide are consistent with many real biological patterns. Here, we placed emphasis on Turing systems, which generate patterns from feedback interaction between processes that on their own have limited pattern-forming ability. We argue

that such mechanisms likely evolved to solve challenges of multicellularity and over time have become essential drivers of diverse pattern-forming events in modern-day animals. Turing famously suggested that complex patterns could arise from a simple system of two reacting and diffusing chemicals. He recognized, however, that biological patterns rarely arise from homogeneity but, rather, develop sequentially, building complexity. The provided examples here of such patterning processes support this idea and offer insights into why such robust patterns may be selected by evolution.

Traditionally, those concerned with identifying cellular and molecular equivalents of Turing model components have been developmental biologists seeking to explain embryonic patterns. Increasingly, however, pattern self-organization has come into the focus of translational biologists studying disease pathogenesis, stem cell biologists striving to increase organoid reproducibility, and synthetic biologists aiming to design sophisticated artificial patterns. This is an exciting time when we can expect to see scientists working in these disparate fields build upon shared knowledge to inspire unconventional solutions to outstanding challenges in pattern formation and control. We anticipate rapid progress along at least three avenues. First, we foresee advances in synthetic patterns. Current examples of engineered patterns, although impressive, are inferior to real animal patterns. More complex patterns will arise when multiple molecular engineering modalities—synthetic morphogens, adhesion code, etc.—will be integrated into networks. Linking them into a sequence may also require engineering epigenetic cell memory so that the identity of cells participating in pattern generation can be progressively and stably restricted in time and space. Second, we anticipate advances in organoid technologies. Future use of signal organizing centers will become more prevalent and sophisticated. Moreover, integrating feedback from cells within organoids to organizing centers will enable responsive control over organoid size, pattern, and cell-type composition. Third, closer fusion between material science, synthetic biology, and stem cell biology may enable creation of next-generation organoids with non-native architectures and functions, a kind of biobots capable of migrating, swarming, and interacting with tissues upon delivery *in vivo*.[101] Meaningful progress in all three of these areas will critically depend on (1) developing a deeper understanding of how information "flows" at all levels of natural pattern-forming processes and on (2) identifying new entry points for synthetic control technologies within such patterning mechanisms. At present, we can deploy pattern-forming control mechanisms reasonably well in model cell lines cultured on plastic and with the aid of cell-cell contact-dependent synthetic molecules (e.g., synNotch system). Yet, our ability to implement synthetic patterns to the degree of complexity and diversity of *in vivo* patterns will also require (1) an ability to produce controlled gradients of soluble molecules, as such gradients are central to natural pattern formation in animal tissues and (2) knowledge on how to reliably connect extracellular signaling inputs with intracellular gene regulatory networks essential for feedback regulation and long-term cellular memory. For these advances to occur, collaborative efforts across a broad spectrum of biological and mathematical disciplines—a systems biology approach—will be essential. As evidenced by this review, many such interdisciplinary efforts are already underway. We hope that the kaleidoscope of fascinating patterns of the natural world presented in this review will help inspire readers from diverse backgrounds find each other and join forces, bringing new knowledge to light by parsing patterns ever more deeply.

ACKNOWLEDGMENTS

M.V.P. is supported by LEO Foundation grants LF-AW-RAM-19-400008 and LF-OC-20-000611; Chan Zuckerberg Initiative grant AN-0000000062; W.M. Keck Foundation grant WMKF-5634988; NSF grant DMS1951144; and NIH grants R01-AR079470, R01-AR079150, R21-AR078939, and P30-AR075047. L.M. is supported by NIH grant R35-GM138256, NSF grants CBET-2034495 and CBET-2145528, and Chan Zuckerberg Initiative grant 2023-332386. A.D.L. is supported by NIH grants U54-CA217378 and R01-HL138659. M.V.P. and A.D.L. are additionally supported by the NSF-Simons Center for Multiscale Fate Research at UC Irvine. C.-M.C. is supported by NIH grants R37-AR060306 and R01-AR047364.

DECLARATION OF INTERESTS

The authors declare no competing interests.

REFERENCES

1. Chuong, C.M., and Richardson, M.K. (2009). Pattern formation today. Int. J. Dev. Biol. *53*, 653–658. https://doi.org/10.1387/ijdb.082594cc.
2. Turing, A.M. (1952). The Chemical Basis of Morphogenesis. Philos T Roy Soc B *237*, 37–72. https://doi.org/10.1098/rstb.1952.0012.
3. Kaelin, C.B., Xu, X., Hong, L.Z., David, V.A., McGowan, K.A., Schmidt-Küntzel, A., Roelke, M.E., Pino, J., Pontius, J., Cooper, G.M., et al. (2012). Specifying and sustaining pigmentation patterns in domestic and wild cats. Science *337*, 1536–1541. https://doi.org/10.1126/science.1220893.
4. Manukyan, L., Montandon, S.A., Fofonjka, A., Smirnov, S., and Milinkovitch, M.C. (2017). A living mesoscopic cellular automaton made of skin scales. Nature *544*, 173–179. https://doi.org/10.1038/nature22031.
5. Glover, J.D., Sudderick, Z.R., Shih, B.B.J., Batho-Samblas, C., Charlton, L., Krause, A.L., Anderson, C., Riddell, J., Balic, A., Li, J., et al. (2023). The developmental basis of fingerprint pattern formation and variation. Cell *186*, 940–956.e20. https://doi.org/10.1016/j.cell.2023.01.015.
6. Murray, J.D. (1989). Mathematical Biology (Springer-Verlag).
7. Sick, S., Reinker, S., Timmer, J., and Schlake, T. (2006). WNT and DKK determine hair follicle spacing through a reaction-diffusion mechanism. Science *314*, 1447–1450. https://doi.org/10.1126/science.1130088.
8. Kaelin, C.B., McGowan, K.A., and Barsh, G.S. (2021). Developmental genetics of color pattern establishment in cats. Nat. Commun. *12*, 5127. https://doi.org/10.1038/s41467-021-25348-2.
9. Mallarino, R., Henegar, C., Mirasierra, M., Manceau, M., Schradin, C., Vallejo, M., Beronja, S., Barsh, G.S., and Hoekstra, H.E. (2016). Developmental mechanisms of stripe patterns in rodents. Nature *539*, 518–523. https://doi.org/10.1038/nature20109.
10. Haupaix, N., Curantz, C., Bailleul, R., Beck, S., Robic, A., and Manceau, M. (2018). The periodic coloration in birds forms through a prepattern of somite origin. Science *361*, eaar4777. https://doi.org/10.1126/science.aar4777.
11. Hiscock, T.W., and Megason, S.G. (2015). Orientation of Turing-like Patterns by Morphogen Gradients and Tissue Anisotropies. Cell Syst. *1*, 408–416. https://doi.org/10.1016/j.cels.2015.12.001.
12. Lin, S.J., Foley, J., Jiang, T.X., Yeh, C.Y., Wu, P., Foley, A., Yen, C.M., Huang, Y.C., Cheng, H.C., Chen, C.F., et al. (2013). Topology of feather melanocyte progenitor niche allows complex pigment patterns to

emerge. Science *340*, 1442–1445. https://doi.org/10.1126/science.1230374.

13. Kondo, S., Watanabe, M., and Miyazawa, S. (2021). Studies of Turing pattern formation in zebrafish skin. Philos. Trans. A Math. Phys. Eng. Sci. *379*, 20200274. https://doi.org/10.1098/rsta.2020.0274.
14. Nakamasu, A., Takahashi, G., Kanbe, A., and Kondo, S. (2009). Interactions between zebrafish pigment cells responsible for the generation of Turing patterns. Proc. Natl. Acad. Sci. USA *106*, 8429–8434. https://doi.org/10.1073/pnas.0808622106.
15. Fofonjka, A., and Milinkovitch, M.C. (2021). Reaction-diffusion in a growing 3D domain of skin scales generates a discrete cellular automaton. Nat. Commun. *12*, 2433. https://doi.org/10.1038/s41467-021-22525-1.
16. Lander, A.D. (2011). Pattern, growth, and control. Cell *144*, 955–969. https://doi.org/10.1016/j.cell.2011.03.009.
17. Lander, A.D., Lo, W.C., Nie, Q., and Wan, F.Y.M. (2009). The measure of success: constraints, objectives, and tradeoffs in morphogen-mediated patterning. Cold Spring Harb. Perspect. Biol. *1*, a002022. https://doi.org/10.1101/cshperspect.a002022.
18. Ben-Moshe, S., and Itzkovitz, S. (2019). Spatial heterogeneity in the mammalian liver. Nat. Rev. Gastroenterol. Hepatol. *16*, 395–410. https://doi.org/10.1038/s41575-019-0134-x.
19. Jimenez, F., and Ruifernández, J.M. (1999). Distribution of human hair in follicular units. A mathematical model for estimating the donor size in follicular unit transplantation. Dermatol. Surg. *25*, 294–298. https://doi.org/10.1046/j.1524-4725.1999.08114.x.
20. Ito, M., Yang, Z., Andl, T., Cui, C., Kim, N., Millar, S.E., and Cotsarelis, G. (2007). Wnt-dependent de novo hair follicle regeneration in adult mouse skin after wounding. Nature *447*, 316–320. https://doi.org/10.1038/nature05766.
21. Yue, Z., Jiang, T.X., Widelitz, R.B., and Chuong, C.M. (2006). Wnt3a gradient converts radial to bilateral feather symmetry via topological arrangement of epithelia. Proc. Natl. Acad. Sci. USA *103*, 951–955. https://doi.org/10.1073/pnas.0506894103.
22. Li, A., Figueroa, S., Jiang, T.X., Wu, P., Widelitz, R., Nie, Q., and Chuong, C.M. (2017). Diverse feather shape evolution enabled by coupling anisotropic signalling modules with self-organizing branching programme. Nat. Commun. *8*, ncomms14139. https://doi.org/10.1038/ncomms14139.
23. Busby, L., Aceituno, C., McQueen, C., Rich, C.A., Ros, M.A., and Towers, M. (2020). Sonic hedgehog specifies flight feather positional information in avian wings. Development *147*, dev188821. https://doi.org/10.1242/dev.188821.
24. Barron, L., Sun, R.C., Aladegbami, B., Erwin, C.R., Warner, B.W., and Guo, J. (2017). Intestinal Epithelial-Specific mTORC1 Activation Enhances Intestinal Adaptation After Small Bowel Resection. Cell. Mol. Gastroenterol. Hepatol. *3*, 231–244. https://doi.org/10.1016/j.jcmgh.2016.10.006.
25. Chen, L., Toke, N.H., Luo, S., Vasoya, R.P., Fullem, R.L., Parthasarathy, A., Perekatt, A.O., and Verzi, M.P. (2019). A reinforcing HNF4-SMAD4 feed-forward module stabilizes enterocyte identity. Nat. Genet. *51*, 777–785. https://doi.org/10.1038/s41588-019-0384-0.
26. Rocha, A.S., Vidal, V., Mertz, M., Kendall, T.J., Charlet, A., Okamoto, H., and Schedl, A. (2015). The Angiocrine Factor Rspondin3 Is a Key Determinant of Liver Zonation. Cell Rep. *13*, 1757–1764. https://doi.org/10.1016/j.celrep.2015.10.049.
27. Pigolotti, S., Krishna, S., and Jensen, M.H. (2007). Oscillation patterns in negative feedback loops. Proc. Natl. Acad. Sci. USA *104*, 6533–6537. https://doi.org/10.1073/pnas.0610759104.
28. Takahashi, J.S. (2017). Transcriptional architecture of the mammalian circadian clock. Nat. Rev. Genet. *18*, 164–179. https://doi.org/10.1038/nrg.2016.150.
29. Loose, M., Fischer-Friedrich, E., Ries, J., Kruse, K., and Schwille, P. (2008). Spatial regulators for bacterial cell division self-organize into surface waves in vitro. Science *320*, 789–792. https://doi.org/10.1126/science.1154413.
30. van Haastert, P.J.M., Keizer-Gunnink, I., Pots, H., Ortiz-Mateos, C., Veltman, D., van Egmond, W., and Kortholt, A. (2021). Forty-five years of cGMP research in Dictyostelium: understanding the regulation and function of the cGMP pathway for cell movement and chemotaxis. Mol. Biol. Cell *32*, ar8. https://doi.org/10.1091/mbc.E21-04-0171.
31. Schaap, P., and Wang, M. (1986). Interactions between adenosine and oscillatory cAMP signaling regulate size and pattern in Dictyostelium. Cell *45*, 137–144. https://doi.org/10.1016/0092-8674(86)90545-3.
32. Rüdiger, S., Míguez, D.G., Muñuzuri, A.P., Sagués, F., and Casademunt, J. (2003). Dynamics of Turing patterns under spatiotemporal forcing. Phys. Rev. Lett. *90*, 128301. https://doi.org/10.1103/PhysRevLett.90.128301.
33. Krause, A.L., Gaffney, E.A., Maini, P.K., and Klika, V. (2021). Modern perspectives on near-equilibrium analysis of Turing systems. Philos. Trans. A Math. Phys. Eng. Sci. *379*, 20200268. https://doi.org/10.1098/rsta.2020.0268.
34. Maini, P.K., Woolley, T.E., Baker, R.E., Gaffney, E.A., and Lee, S.S. (2012). Turing's model for biological pattern formation and the robustness problem. Interface Focus *2*, 487–496. https://doi.org/10.1098/rsfs.2011.0113.
35. Glover, J.D., Wells, K.L., Matthäus, F., Painter, K.J., Ho, W., Riddell, J., Johansson, J.A., Ford, M.J., Jahoda, C.A.B., Klika, V., et al. (2017). Hierarchical patterning modes orchestrate hair follicle morphogenesis. PLoS Biol. *15*, e2002117. https://doi.org/10.1371/journal.pbio.2002117.
36. Zheng, Y., Du, X., Wang, W., Boucher, M., Parimoo, S., and Stenn, K. (2005). Organogenesis from dissociated cells: generation of mature cycling hair follicles from skin-derived cells. J. Invest. Dermatol. *124*, 867–876. https://doi.org/10.1111/j.0022-202X.2005.23716.x.
37. Painter, K.J., Ptashnyk, M., and Headon, D.J. (2021). Systems for intricate patterning of the vertebrate anatomy. Philos. Trans. A Math. Phys. Eng. Sci. *379*, 20200270. https://doi.org/10.1098/rsta.2020.0270.
38. Cheng, C.W., Niu, B., Warren, M., Pevny, L.H., Lovell-Badge, R., Hwa, T., and Cheah, K.S.E. (2014). Predicting the spatiotemporal dynamics of hair follicle patterns in the developing mouse. Proc. Natl. Acad. Sci. USA *111*, 2596–2601. https://doi.org/10.1073/pnas.1313083111.
39. Bailleul, R., Curantz, C., Desmarquet-Trin Dinh, C., Hidalgo, M., Touboul, J., and Manceau, M. (2019). Symmetry breaking in the embryonic skin triggers directional and sequential plumage patterning. PLoS Biol. *17*, e3000448. https://doi.org/10.1371/journal.pbio.3000448.
40. Ho, W.K.W., Freem, L., Zhao, D., Painter, K.J., Woolley, T.E., Gaffney, E.A., McGrew, M.J., Tzika, A., Milinkovitch, M.C., Schneider, P., et al. (2019). Feather arrays are patterned by interacting signalling and cell density waves. PLoS Biol. *17*, e3000132. https://doi.org/10.1371/journal.pbio.3000132.
41. Wu, X.S., Yeh, C.Y., Harn, H.I.C., Jiang, T.X., Wu, P., Widelitz, R.B., Baker, R.E., and Chuong, C.M. (2019). Self-assembly of biological networks via adaptive patterning revealed by avian intradermal muscle network formation. Proc. Natl. Acad. Sci. USA *116*, 10858–10867. https://doi.org/10.1073/pnas.1818506116.
42. Yum, S.M., Baek, I.K., Hong, D., Kim, J., Jung, K., Kim, S., Eom, K., Jang, J., Kim, S., Sattorov, M., et al. (2020). Fingerprint ridges allow primates to regulate grip. Proc. Natl. Acad. Sci. USA *117*, 31665–31673. https://doi.org/10.1073/pnas.2001055117.
43. Raspopovic, J., Marcon, L., Russo, L., and Sharpe, J. (2014). Modeling digits. Digit patterning is controlled by a Bmp-Sox9-Wnt Turing network modulated by morphogen gradients. Science *345*, 566–570. https://doi.org/10.1126/science.1252960.
44. Litingtung, Y., Dahn, R.D., Li, Y., Fallon, J.F., and Chiang, C. (2002). Shh and Gli3 are dispensable for limb skeleton formation but regulate digit

number and identity. Nature *418*, 979–983. https://doi.org/10.1038/nature01033.

45. Sheth, R., Marcon, L., Bastida, M.F., Junco, M., Quintana, L., Dahn, R., Kmita, M., Sharpe, J., and Ros, M.A. (2012). Hox genes regulate digit patterning by controlling the wavelength of a Turing-type mechanism. Science *338*, 1476–1480. https://doi.org/10.1126/science.1226804.
46. Davis, M.C., Dahn, R.D., and Shubin, N.H. (2007). An autopodial-like pattern of Hox expression in the fins of a basal actinopterygian fish. Nature *447*, 473–476. https://doi.org/10.1038/nature05838.
47. Salazar-Ciudad, I., and Jernvall, J. (2002). A gene network model accounting for development and evolution of mammalian teeth. Proc. Natl. Acad. Sci. USA *99*, 8116–8120. https://doi.org/10.1073/pnas.132069499.
48. Hunter, J.P., and Jernvall, J. (1995). The hypocone as a key innovation in mammalian evolution. Proc. Natl. Acad. Sci. USA *92*, 10718–10722. https://doi.org/10.1073/pnas.92.23.10718.
49. Couzens, A.M.C., Sears, K.E., and Rücklin, M. (2021). Developmental influence on evolutionary rates and the origin of placental mammal tooth complexity. Proc. Natl. Acad. Sci. USA *118*, e2019294118. https://doi.org/10.1073/pnas.2019294118.
50. Wolfram, S. (1983). Statistical mechanics of cellular automata. Rev. Mod. Phys. *55*, 601–644. https://doi.org/10.1103/RevModPhys.55.601.
51. Plikus, M.V., and Chuong, C.M. (2008). Complex hair cycle domain patterns and regenerative hair waves in living rodents. J. Invest. Dermatol. *128*, 1071–1080. https://doi.org/10.1038/sj.jid.5701180.
52. Joost, S., Annusver, K., Jacob, T., Sun, X., Dalessandri, T., Sivan, U., Sequeira, I., Sandberg, R., and Kasper, M. (2020). The Molecular Anatomy of Mouse Skin during Hair Growth and Rest. Cell Stem Cell *26*, 441–457.e7. https://doi.org/10.1016/j.stem.2020.01.012.
53. Plikus, M.V., Baker, R.E., Chen, C.C., Fare, C., de la Cruz, D., Andl, T., Maini, P.K., Millar, S.E., Widelitz, R., and Chuong, C.M. (2011). Self-organizing and stochastic behaviors during the regeneration of hair stem cells. Science *332*, 586–589. https://doi.org/10.1126/science.1201647.
54. Plikus, M.V., Mayer, J.A., de la Cruz, D., Baker, R.E., Maini, P.K., Maxson, R., and Chuong, C.M. (2008). Cyclic dermal BMP signalling regulates stem cell activation during hair regeneration. Nature *451*, 340–344. https://doi.org/10.1038/nature06457.
55. Packard, N.H., and Wolfram, S. (1985). Two-dimensional cellular automata. J. Stat. Phys. *38*, 901–946. https://doi.org/10.1007/BF01010423.
56. Chen, C.C., Murray, P.J., Jiang, T.X., Plikus, M.V., Chang, Y.T., Lee, O.K., Widelitz, R.B., and Chuong, C.M. (2014). Regenerative hair waves in aging mice and extra-follicular modulators follistatin, dkk1, and sfrp4. J. Invest. Dermatol. *134*, 2086–2096. https://doi.org/10.1038/jid.2014.139.
57. Wang, Q., Oh, J.W., Lee, H.L., Dhar, A., Peng, T., Ramos, R., Guerrero-Juarez, C.F., Wang, X., Zhao, R., Cao, X., et al. (2017). A multi-scale model for hair follicles reveals heterogeneous domains driving rapid spatiotemporal hair growth patterning. Elife *6*, e22772. https://doi.org/10.7554/eLife.22772.
58. Chen, C.C., Wang, L., Plikus, M.V., Jiang, T.X., Murray, P.J., Ramos, R., Guerrero-Juarez, C.F., Hughes, M.W., Lee, O.K., Shi, S., et al. (2015). Organ-level quorum sensing directs regeneration in hair stem cell populations. Cell *161*, 277–290. https://doi.org/10.1016/j.cell.2015.02.016.
59. Harn, H.I.C., Wang, S.P., Lai, Y.C., Van Handel, B., Liang, Y.C., Tsai, S., Schiessl, I.M., Sarkar, A., Xi, H., Hughes, M., et al. (2021). Symmetry breaking of tissue mechanics in wound induced hair follicle regeneration of laboratory and spiny mice. Nat. Commun. *12*, 2595. https://doi.org/10.1038/s41467-021-22822-9.
60. Lim, C.H., Sun, Q., Ratti, K., Lee, S.H., Zheng, Y., Takeo, M., Lee, W., Rabbani, P., Plikus, M.V., Cain, J.E., et al. (2018). Hedgehog stimulates hair follicle neogenesis by creating inductive dermis during murine skin wound healing. Nat. Commun. *9*, 4903. https://doi.org/10.1038/s41467-018-07142-9.
61. Gay, D., Kwon, O., Zhang, Z., Spata, M., Plikus, M.V., Holler, P.D., Ito, M., Yang, Z., Treffeisen, E., Kim, C.D., et al. (2013). Fgf9 from dermal γδ T cells induces hair follicle neogenesis after wounding. Nat. Med. *19*, 916–923. https://doi.org/10.1038/nm.3181.
62. Gay, D., Ghinatti, G., Guerrero-Juarez, C.F., Ferrer, R.A., Ferri, F., Lim, C.H., Murakami, S., Gault, N., Barroca, V., Rombeau, I., et al. (2020). Phagocytosis of Wnt inhibitor SFRP4 by late wound macrophages drives chronic Wnt activity for fibrotic skin healing. Sci. Adv. *6*, eaay3704. https://doi.org/10.1126/sciadv.aay3704.
63. Wang, B., Sinha, T., Jiao, K., Serra, R., and Wang, J. (2011). Disruption of PCP signaling causes limb morphogenesis and skeletal defects and may underlie Robinow syndrome and brachydactyly type B. Hum. Mol. Genet. *20*, 271–285. https://doi.org/10.1093/hmg/ddq462.
64. Rongioletti, F., Fausti, V., and Parodi, A. (2014). Erythema gyratum repens is not an obligate paraneoplastic disease: a systematic review of the literature and personal experience. J. Eur. Acad. Dermatol. Venereol. *28*, 112–115. https://doi.org/10.1111/j.1468-3083.2012.04663.x.
65. Eubanks, L.E., McBurney, E., and Reed, R. (2001). Erythema gyratum repens. Am. J. Med. Sci. *321*, 302–305. https://doi.org/10.1097/00000441-200105000-00002.
66. Glitzner, E., Korosec, A., Brunner, P.M., Drobits, B., Amberg, N., Schonthaler, H.B., Kopp, T., Wagner, E.F., Stingl, G., Holcmann, M., and Sibilia, M. (2014). Specific roles for dendritic cell subsets during initiation and progression of psoriasis. EMBO Mol. Med. *6*, 1312–1327. https://doi.org/10.15252/emmm.201404114.
67. Lowes, M.A., Kikuchi, T., Fuentes-Duculan, J., Cardinale, I., Zaba, L.C., Haider, A.S., Bowman, E.P., and Krueger, J.G. (2008). Psoriasis vulgaris lesions contain discrete populations of Th1 and Th17 T cells. J. Invest. Dermatol. *128*, 1207–1211. https://doi.org/10.1038/sj.jid.5701213.
68. Ringham, L., Prusinkiewicz, P., and Gniadecki, R. (2019). Skin Patterning in Psoriasis by Spatial Interactions between Pathogenic Cytokines. iScience *20*, 546–553. https://doi.org/10.1016/j.isci.2019.10.008.
69. Langley, R.G., Sofen, H., Dei-Cas, I., Reich, K., Sigurgeirsson, B., Warren, R.B., Paul, C., Szepietowski, J.C., Tsai, T.F., Hampele, I., et al. (2023). Secukinumab long-term efficacy and safety in psoriasis through to year 5 of treatment: results of a randomized extension of the phase III ERASURE and FIXTURE trials. Br. J. Dermatol. *188*, 198–207. https://doi.org/10.1093/bjd/ljac040.
70. Reich, K., Armstrong, A.W., Langley, R.G., Flavin, S., Randazzo, B., Li, S., Hsu, M.C., Branigan, P., and Blauvelt, A. (2019). Guselkumab versus secukinumab for the treatment of moderate-to-severe psoriasis (ECLIPSE): results from a phase 3, randomised controlled trial. Lancet *394*, 831–839. https://doi.org/10.1016/S0140-6736(19)31773-8.
71. van den Boorn, J.G., Konijnenberg, D., Dellemijn, T.A.M., van der Veen, J.P.W., Bos, J.D., Melief, C.J.M., Vyth-Dreese, F.A., and Luiten, R.M. (2009). Autoimmune destruction of skin melanocytes by perilesional T cells from vitiligo patients. J. Invest. Dermatol. *129*, 2220–2232. https://doi.org/10.1038/jid.2009.32.
72. Harris, J.E., Harris, T.H., Weninger, W., Wherry, E.J., Hunter, C.A., and Turka, L.A. (2012). A mouse model of vitiligo with focused epidermal depigmentation requires IFN-γ for autoreactive $CD8^+$ T-cell accumulation in the skin. J. Invest. Dermatol. *132*, 1869–1876. https://doi.org/10.1038/jid.2011.463.
73. Rashighi, M., Agarwal, P., Richmond, J.M., Harris, T.H., Dresser, K., Su, M.W., Zhou, Y., Deng, A., Hunter, C.A., Luster, A.D., and Harris, J.E. (2014). CXCL10 is critical for the progression and maintenance of depigmentation in a mouse model of vitiligo. Sci. Transl. Med. *6*, 223ra23. https://doi.org/10.1126/scitranslmed.3007811.
74. Sheikh, A., Rafique, W., Owais, R., Malik, F., and Ali, E. (2022). FDA approves Ruxolitinib (Opzelura) for Vitiligo Therapy: A breakthrough in the field of dermatology. Ann. Med. Surg. *81*, 104499. https://doi.org/10.1016/j.amsu.2022.104499.
75. Xu, Z., Chen, D., Hu, Y., Jiang, K., Huang, H., Du, Y., Wu, W., Wang, J., Sui, J., Wang, W., et al. (2022). Anatomically distinct fibroblast subsets

determine skin autoimmune patterns. Nature *601*, 118–124. https://doi.org/10.1038/s41586-021-04221-8.

76. Pratt, C.H., King, L.E., Jr., Messenger, A.G., Christiano, A.M., and Sundberg, J.P. (2017). Alopecia areata. Nat. Rev. Dis. Primers *3*, 17011. https://doi.org/10.1038/nrdp.2017.11.
77. Paus, R., and Bertolini, M. (2013). The role of hair follicle immune privilege collapse in alopecia areata: status and perspectives. J. Investig. Dermatol. Symp. Proc. *16*, S25–S27. https://doi.org/10.1038/jidsymp.2013.7.
78. Xing, L., Dai, Z., Jabbari, A., Cerise, J.E., Higgins, C.A., Gong, W., de Jong, A., Harel, S., DeStefano, G.M., Rothman, L., et al. (2014). Alopecia areata is driven by cytotoxic T lymphocytes and is reversed by JAK inhibition. Nat. Med. *20*, 1043–1049. https://doi.org/10.1038/nm.3645.
79. Daley, G.Q. (2008). Common themes of dedifferentiation in somatic cell reprogramming and cancer. Cold Spring Harb. Symp. Quant. Biol. *73*, 171–174. https://doi.org/10.1101/sqb.2008.73.041.
80. Snir, O.L., DeJoseph, M., Wong, S., Buza, N., and Hui, P. (2017). Frequent homozygosity in both mature and immature ovarian teratomas: a shared genetic basis of tumorigenesis. Mod. Pathol. *30*, 1467–1475. https://doi.org/10.1038/modpathol.2017.66.
81. Northcott, P.A., Jones, D.T.W., Kool, M., Robinson, G.W., Gilbertson, R.J., Cho, Y.J., Pomeroy, S.L., Korshunov, A., Lichter, P., Taylor, M.D., and Pfister, S.M. (2012). Medulloblastomics: the end of the beginning. Nat. Rev. Cancer *12*, 818–834. https://doi.org/10.1038/nrc3410.
82. Luo, Z., Zhou, X., Mandal, K., He, N., Wennerberg, W., Qu, M., Jiang, X., Sun, W., and Khademhosseini, A. (2021). Reconstructing the tumor architecture into organoids. Adv. Drug Deliv. Rev. *176*, 113839. https://doi.org/10.1016/j.addr.2021.113839.
83. Lee, Y., Lee, J.K., Ahn, S.H., Lee, J., and Nam, D.H. (2016). WNT signaling in glioblastoma and therapeutic opportunities. Lab. Invest. *96*, 137–150. https://doi.org/10.1038/labinvest.2015.140.
84. Werner, S., Vu, H.T.K., and Rink, J.C. (2017). Self-organization in development, regeneration and organoids. Curr. Opin. Cell Biol. *44*, 102–109. https://doi.org/10.1016/j.ceb.2016.09.002.
85. Takebe, T., and Wells, J.M. (2019). Organoids by design. Science *364*, 956–959. https://doi.org/10.1126/science.aaw7567.
86. Basu, S., Gerchman, Y., Collins, C.H., Arnold, F.H., and Weiss, R. (2005). A synthetic multicellular system for programmed pattern formation. Nature *434*, 1130–1134. https://doi.org/10.1038/nature03461.
87. Martínez-Ara, G., Stapornwongkul, K.S., and Ebisuya, M. (2022). Scaling up complexity in synthetic developmental biology. Science *378*, 864–868. https://doi.org/10.1126/science.add9666.
88. Ho, C., and Morsut, L. (2021). Novel synthetic biology approaches for developmental systems. Stem Cell Rep. *16*, 1051–1064. https://doi.org/10.1016/j.stemcr.2021.04.007.
89. Sekine, R., Shibata, T., and Ebisuya, M. (2018). Synthetic mammalian pattern formation driven by differential diffusivity of Nodal and Lefty. Nat. Commun. *9*, 5456. https://doi.org/10.1038/s41467-018-07847-x.
90. Manhas, J., Edelstein, H.I., Leonard, J.N., and Morsut, L. (2022). The evolution of synthetic receptor systems. Nat. Chem. Biol. *18*, 244–255. https://doi.org/10.1038/s41589-021-00926-z.
91. Morsut, L., Roybal, K.T., Xiong, X., Gordley, R.M., Coyle, S.M., Thomson, M., and Lim, W.A. (2016). Engineering Customized Cell Sensing and Response Behaviors Using Synthetic Notch Receptors. Cell *164*, 780–791. https://doi.org/10.1016/j.cell.2016.01.012.
92. Toda, S., McKeithan, W.L., Hakkinen, T.J., Lopez, P., Klein, O.D., and Lim, W.A. (2020). Engineering synthetic morphogen systems that can program multicellular patterning. Science *370*, 327–331. https://doi.org/10.1126/science.abc0033.
93. Santorelli, M., Bhamidipati, P.S., Kavanagh, A., MacKrell, V.A., Sondkar, T., Thomson, M., and Morsut, L. (2022). Control of spatio-temporal patterning via cell density in a multicellular synthetic gene circuit. bioRxiv. https://doi.org/10.1101/2022.10.04.510900.
94. Toda, S., Blauch, L.R., Tang, S.K.Y., Morsut, L., and Lim, W.A. (2018). Programming self-organizing multicellular structures with synthetic cell-cell signaling. Science *361*, 156–162. https://doi.org/10.1126/science.aat0271.
95. Cederquist, G.Y., Asciolla, J.J., Tchieu, J., Walsh, R.M., Cornacchia, D., Resh, M.D., and Studer, L. (2019). Specification of positional identity in forebrain organoids. Nat. Biotechnol. *37*, 436–444. https://doi.org/10.1038/s41587-019-0085-3.
96. Anand, G.M., Megale, H.C., Murphy, S.H., Weis, T., Lin, Z., He, Y., Wang, X., Liu, J., and Ramanathan, S. (2023). Controlling organoid symmetry breaking uncovers an excitable system underlying human axial elongation. Cell *186*, 497–512.e23. https://doi.org/10.1016/j.cell.2022.12.043.
97. Yaman, Y.I., and Ramanathan, S. (2023). Controlling human organoid symmetry breaking reveals signaling gradients drive segmentation clock waves. Cell *186*, 513–527.e19. https://doi.org/10.1016/j.cell.2022.12.042.
98. Rivron, N.C., Martinez Arias, A., Pera, M.F., Moris, N., and M'Hamdi, H.,I. (2023). An ethical framework for human embryology with embryo models. Cell *186*, 3548–3557. https://doi.org/10.1016/j.cell.2023.07.028.
99. Liu, X., and Polo, J.M. (2024). Human blastoid as an in vitro model of human blastocysts. Curr. Opin. Genet. Dev. *84*, 102135. https://doi.org/10.1016/j.gde.2023.102135.
100. Karvas, R.M., Zemke, J.E., Ali, S.S., Upton, E., Sane, E., Fischer, L.A., Dong, C., Park, K.M., Wang, F., Park, K., et al. (2023). 3D-cultured blastoids model human embryogenesis from pre-implantation to early gastrulation stages. Cell Stem Cell *30*, 1148–1165.e7. https://doi.org/10.1016/j.stem.2023.08.005.
101. Gumuskaya, G., Srivastava, P., Cooper, B.G., Lesser, H., Semegran, B., Garnier, S., and Levin, M. (2024). Motile Living Biobots Self-Construct from Adult Human Somatic Progenitor Seed Cells. Adv. Sci. *11*, e2303575. https://doi.org/10.1002/advs.202303575.